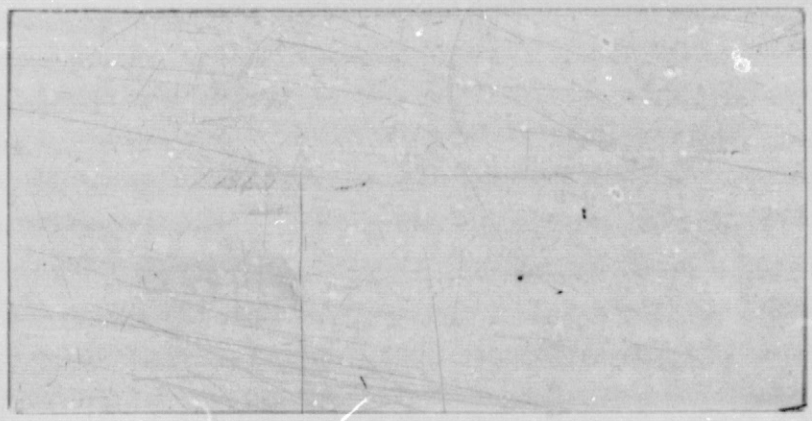

HREC-5712-1
LMSC-HREC D225157

LOCKHEED MISSILES & SPACE COMPANY
HUNTSVILLE RESEARCH & ENGINEERING CENTER
HUNTSVILLE RESEARCH PARK
4800 BRADFORD DRIVE, HUNTSVILLE, ALABAMA

STUDY ON PROPELLANT DYNAMICS DURING DOCKING

INTERIM REPORT

June 1971

Contract NAS8-25712

Prepared for National Aeronautics and Space Administration
Marshall Space Flight Center, Alabama 35812

by

G. C. Feng
S. J. Robertson

APPROVED:

B. Hobson Shirley

B. Hobson Shirley, Supervisor
Aerophysics Section

George D. Reny

George D. Reny, Manager
Aeromechanics Department

J. S. Farrior

J. S. Farrior
Resident Director

FOREWORD

This document presents an interim report of a research program performed by Lockheed's Huntsville Research & Engineering Center (Lockheed-Huntsville), while under contract to NASA-Marshall Space Flight Center (NASA-MSFC), Contract NAS8-25712. Technical monitor of the contract is Mr. Frank Bugg, S&E-AERO-DDS.

SUMMARY

A modification of the Marker-and-Cell (MAC) computing technique was developed to calculate the two-dimensional or axisymmetric flow of liquids in fuel tanks of space vehicles during a docking maneuver in orbit. The basic MAC technique was modified to include the capability for treating flows with arbitrary curved boundaries and surface tension effects. In addition the capability was included for computing forces and moments on the tank walls caused by the propellant motion in the tank.

The modified computer program was utilized to calculate the propellant dynamics in two-dimensional and axisymmetric tanks for several specific cases. The use of the program appeared to be generally successful in all cases. Some numerical instabilities developed on the free surface, however, for low viscosity fluids. Other numerical problems appeared in regions of thin liquid layers, such as a trailing tail of liquid moving along the tank boundary. These instabilities appear only in regions near the surface and are apparently unrelated to the numerical stability criteria which apply to all computational cells. An effort is continuing to correct these numerical difficulities.

A preliminary investigation has indicated the probability of a high degree of success in modifying the MAC technique for use in three-dimensional flow conditions. Future effort on this research program will be devoted primarily to this task.

CONTENTS

Section		Page
	FOREWORD	ii
	SUMMARY	iii
1	INTRODUCTION	1
2	FORMULATION	2
	2.1 The Differential Equations	2
	2.2 The Finite Difference Equations	5
	2.3 The SMAC Computing Technique	8
3	NUMERICAL SCHEMES	13
	3.1 The Modified SMAC Computing Technique	13
	3.2 Boundary Conditions	15
	3.3 Surface Tension Effects	18
4	THE COMPUTER PROGRAM	21
5	EXAMPLES	23
6	CONCLUSIONS AND RECOMMENDATIONS	26
	REFERENCES	27
	ILLUSTRATIONS	28

NOMENCLATURE

$\bar{f}$	acceleration due to surface tension force, m/sec^2
$\bar{g}$	equivalent gravitational acceleration, m/sec^2
$\hat{n}$	unit normal of a free surface
p	pressure, N/m^2
(r, z) or (x,y)	coordinates of an axisymmetric or a planar flow, respectively, m
t	time, sec
$\bar{v}$	velocity, m/sec
δr, δz	mesh size of an axisymmetric flow, m
δt	time increment, sec
$\delta \beta$	iteration step, m^2/sec
θ	a known potential function, m^2/sec^2
ν	kinematic viscosity coefficient, m^2/sec
ρ	mass density, kg/m^3
τ	surface tension coefficient, N/m^2
φ	p/ρ = velocity potential, m^2/sec^2
ψ	potential function, m^2/sec

Section 1
INTRODUCTION

Projected Space Shuttle missions include the rendezvous and docking in orbit with permanent space stations or other orbiting vehicles. On many of its planned missions, the Space Shuttle orbiter vehicle will be transporting a cargo of liquid propellants or life support cryogenic fluids. The motion of these fluids within their containers will exert forces and moments which must be reckoned with in the design of the docking mechanism, control system, and procedures for the docking maneuver.

Most previous analytical studies of propellant dynamics were concerned with the relatively low amplitude slosh encountered during powered flight. The large amplitude motions, typical of low gravity conditions, such as propellant reorientation from one end of the tank to the other, have presented formidable mathematical difficulties. These difficulties have been partially overcome in recent years through the use of numerical techniques utilizing high speed digital computers. One such technique is the Marker-and-Cell (MAC) technique described in Refs. 1 and 2.

A research effort has been undertaken to develop a satisfactory analytical tool for computing the motion of liquids in their containers under low gravity conditions. The application of this analytical tool will be the prediction of forces and moments on the tank wall during the docking maneuver of Space Shuttle vehicles. The approach taken is to modify the MAC technique for use in this application. This interim report describes the results obtained during the first 12 months of this research program.

Section 2
FORMULATION

2.1 THE DIFFERENTIAL EQUATIONS

The differential equations which govern the transient flow of a viscous incompressible fluid are

$$\frac{\partial \bar{v}}{\partial t} = -(\bar{v}\cdot\nabla)\,\bar{v} - \nabla\varphi + \nu\nabla^2\bar{v} + \bar{g} + \bar{f} \qquad (1)$$

$$D \equiv \nabla\cdot\bar{v} = 0 \qquad (2)$$

where the vector $\bar{f}$ represents the surface tension effect. It is non-zero only at the free surface of the fluid. Other notations used in Eqs. (1) and (2) are:

$\bar{v}$ = velocity vector

$\varphi = \frac{p}{\rho}$ = velocity potential

p = pressure

ρ = mass density

ν = kinematic viscosity coefficient

$\bar{g}$ = equivalent gravitational acceleration vector.

In an axisymmetric or a planar flow, Eqs. (1) and (2) can be reduced to the following forms (Ref. 2):

Axisymmetric

$$\frac{\partial v_r}{\partial t} = -\frac{1}{r}\frac{\partial}{\partial r}(r v_r^2) - \frac{\partial}{\partial z}(v_r v_z) - \frac{\partial \varphi}{\partial r} + \nu \frac{\partial}{\partial z}\left(\frac{\partial v_r}{\partial z} - \frac{\partial v_z}{\partial r}\right) + g_r + f_r \qquad (3)$$

$$\frac{\partial v_z}{\partial t} = -\frac{1}{r}\frac{\partial}{\partial r}(r v_r v_z) - \frac{\partial}{\partial z}(v_z^2) - \frac{\partial \varphi}{\partial z} - \frac{\nu}{r}\frac{\partial}{\partial r}\left[r\left(\frac{\partial v_r}{\partial z} - \frac{\partial v_z}{\partial r}\right)\right] + g_z + f_z \qquad (4)$$

$$D \equiv \frac{1}{r}\frac{\partial}{\partial r}(r v_r) + \frac{\partial v_z}{\partial z} = 0 \qquad (5)$$

Planar

$$\frac{\partial v_x}{\partial t} = -\frac{\partial}{\partial x}(v_x^2) - \frac{\partial}{\partial y}(v_x v_y) - \frac{\partial \varphi}{\partial x} + \nu \frac{\partial}{\partial y}\left(\frac{\partial v_x}{\partial y} - \frac{\partial v_y}{\partial x}\right) + g_x + f_x \qquad (6)$$

$$\frac{\partial v_y}{\partial t} = -\frac{\partial}{\partial x}(v_x v_y) - \frac{\partial}{\partial y}(v_y^2) - \frac{\partial \varphi}{\partial y} - \nu \frac{\partial}{\partial x}\left(\frac{\partial v_x}{\partial y} - \frac{\partial v_y}{\partial x}\right) + g_y + f_y \qquad (7)$$

$$D \equiv \frac{\partial v_x}{\partial x} + \frac{\partial v_y}{\partial y} = 0\,. \qquad (8)$$

The stress tensors of the two cases are

$$\begin{cases} \sigma_{rr} = -\varphi + \dfrac{2\nu}{r}\dfrac{\partial}{\partial r}(r v_r) \\ \sigma_{zz} = -\varphi + 2\nu \dfrac{\partial v_z}{\partial z} \\ \sigma_{rz} = \nu\left(\dfrac{\partial v_r}{\partial z} + \dfrac{\partial v_z}{\partial r}\right) \end{cases} \qquad (9)$$

and

$$\begin{cases} \sigma_{xx} = -\varphi + 2\nu \dfrac{\partial v_x}{\partial x} \\ \sigma_{yy} = -\varphi + 2\nu \dfrac{\partial v_y}{\partial y} \\ \sigma_{xy} = \nu \left(\dfrac{\partial v_x}{\partial y} + \dfrac{\partial v_y}{\partial x} \right), \end{cases} \tag{10}$$

respectively. Since the two sets of equations are similar and can be solved through the same procedure, subsequent discussions on solution techniques and numerical schemes will be based on an axisymmetric formulation. If the planar case is of interest, it can be readily derived by letting $r \equiv 1$.

In this study, all fluids are considered to be at rest initially, i.e., $\bar{v}(r, z, 0) = p(r, z, 0) = 0$. For flows in a low-g field, the initial free surface of the fluid is assumed to be described by the equation

$$\frac{r^2}{a^2} + \frac{z^2}{b^2} = 1$$

where a and b are the semi-axes of an ellipse. The boundary conditions of the problems to be studied are

$$v_n = \sigma_t = 0 \qquad \text{(at a rigid boundary)} \tag{11}$$

$$\begin{cases} \sigma_n = \sigma(r, z, t) \\ \sigma_t = 0 \qquad \text{(at a free surface)} \end{cases} \tag{12}$$

where a variable with a subscript n or t denotes the normal or tangential component of the variable, respectively, and $\sigma(r, z, t)$ is a known function.

2.2 THE FINITE DIFFERENCE EQUATIONS

Rectangular meshes are employed in writing the finite difference equations of the formulated problem. The velocity components of a fluid are specified at the boundaries of a cell. The pressure and all other quantities of the fluid are specified at the center of a cell (Fig. 1). A set of marker particles will be assigned for tracking the flow field, and they are displaced in accordance with the local velocities after completion of each computing cycle. To facilitate the construction of the numerical scheme and direction of the execution sequence, the following seven types of cells are defined for identifying the status of a cell in a computing cycle (Fig. 2):

1. Empty cell (E): A cell having no marker particle,

2. Boundary cell (B): An empty cell whose boundary forms a portion of the straight boundary of a container,

3. Hybrid empty cell (HE): An empty cell containing a portion of the curved boundary of a container,

4. Surface cell (S): A cell having marker particles and neighboring with at least one empty cell,

5. Hybrid surface cell (HS): A surface cell containing a portion of the curved boundary of a container,

6. Full cell (F): A cell having marker particles and not neighboring with any empty cell,

7. Hybrid full cell (HF): A full cell containing a portion of the curved boundary of a container.

As shown in Fig. 1, the finite difference equations (3), (4) and (5) for a full or surface cell may be written as

$$(v_r^{n+1})_{i+\frac{1}{2},j} = (v_r^n)_{i+\frac{1}{2},j} - \delta t \left\{ \frac{1}{r_{i+\frac{1}{2}}\,\delta r} \left[r_{i+1} (v_r^n)^2_{i+1,j} - r_i (v_r^n)^2_{i,j} \right] \right.$$

$$+ \frac{1}{\delta z} \left[(v_r^n v_z^n)_{i+\frac{1}{2},j+\frac{1}{2}} - (v_r^n v_z^n)_{i+\frac{1}{2},j-\frac{1}{2}} \right] + \frac{1}{\delta r} \left[\varphi_{i+1,j} - \varphi_{i,j} \right]$$

$$- \frac{\nu}{(\delta z)^2} \left[(v_r^n)_{i+\frac{1}{2},j+1} + (v_r^n)_{i+\frac{1}{2},j-1} - 2 (v_r^n)_{i+\frac{1}{2},j} \right]$$

$$+ \frac{\nu}{\delta r\, \delta z} \left[(v_z^n)_{i+1,j+\frac{1}{2}} - (v_z^n)_{i,j+\frac{1}{2}} - (v_z^n)_{i+1,j-\frac{1}{2}} + (v_z^n)_{i,j-\frac{1}{2}} \right]$$

$$\left. - g_r^n - (f_r^n)_{i,j} \right\} \qquad (13)$$

$$(v_z^{n+1})_{i,j+\frac{1}{2}} = (v_z^n)_{i,j+\frac{1}{2}} - \delta t \left\{ \frac{1}{r_i\, \delta r} \left[r_{i+\frac{1}{2}} (v_r^n v_z^n)_{i+\frac{1}{2},j+\frac{1}{2}} - r_{i-\frac{1}{2}} (v_r^n v_z^n)_{i-\frac{1}{2},j+\frac{1}{2}} \right] \right.$$

$$+ \frac{1}{\delta z} \left[(v_z^n)^2_{i,j+1} - (v_z^n)^2_{i,j} \right] + \frac{1}{\delta z} \left[\varphi_{i,j+1} - \varphi_{i,j} \right]$$

$$+ \frac{\nu}{r_i\, \delta r} \left[r_{i+\frac{1}{2}} \left(\frac{(v_r^n)_{i+\frac{1}{2},j+1} - (v_r^n)_{i+\frac{1}{2},j}}{\delta z} - \frac{(v_z^n)_{i+1,j+\frac{1}{2}} - (v_z^n)_{i,j+\frac{1}{2}}}{\delta r} \right) \right.$$

$$\left. - r_{i-\frac{1}{2}} \left(\frac{(v_r^n)_{i-\frac{1}{2},j+1} - (v_r^n)_{i-\frac{1}{2},j}}{\delta z} - \frac{(v_z^n)_{i,j+\frac{1}{2}} - (v_z^n)_{i-1,j+\frac{1}{2}}}{\delta r} \right) \right]$$

$$\left. - g_z^n - (f_z^n)_{i,j} \right\} \qquad (14)$$

$$D_{i,j}^{n+1} \equiv \frac{1}{r_i \delta r}\left[r_{i+\frac{1}{2}}(v_r^{n+1})_{i+\frac{1}{2},j} - r_{i-\frac{1}{2}}(v_r^{n+1})_{i-\frac{1}{2},j}\right] + \frac{1}{\delta z}\left[(v_z^{n+1})_{i,j+\frac{1}{2}} - (v_z^{n+1})_{i,j-\frac{1}{2}}\right] \quad (15)$$

where

$$(v_r^n)^2_{i,j} = (v_r^n)_{i+\frac{1}{2},j}(v_r^n)_{i-\frac{1}{2},j}$$

$$(v_z^n)^2_{i,j} = (v_z^n)_{i,j+\frac{1}{2}}(v_z^n)_{i,j-\frac{1}{2}}$$

$$(v_r^n v_z^n)_{i+\frac{1}{2},j+\frac{1}{2}} = \frac{1}{4}\left[(v_r^n)_{i+\frac{1}{2},j+1} + (v_r^n)_{i+\frac{1}{2},j}\right]\left[(v_z^n)_{i+1,j+\frac{1}{2}} + (v_z^n)_{i,j+\frac{1}{2}}\right].$$

Note that the superscript n of a variable denotes that the variable is evaluated at time $n\,\delta t$. The velocity potential $\varphi_{i,j}$ at time $(n+1)\,\delta t$ is obtained through an iteration process which will be discussed in Sections 2.3 and 3.1. Similarly, the finite difference equations of the stresses in an incompressible fluid may be expressed as

$$(\sigma_{rr}^n)_{i,j} = -\varphi_{i,j} + \frac{2\nu}{r_i \delta r}\left[r_{i+\frac{1}{2}}(v_r^n)_{i+\frac{1}{2},j} - r_{i-\frac{1}{2}}(v_r^n)_{i-\frac{1}{2},j}\right] \quad (16)$$

$$(\sigma_{zz}^n)_{i,j} = -\varphi_{i,j} + \frac{2\nu}{\delta z}\left[(v_z^n)_{i,j+\frac{1}{2}} - (v_z^n)_{i,j-\frac{1}{2}}\right] \quad (17)$$

$$(\sigma_{rz}^n)_{i,j} = \nu\left\{\frac{1}{\delta z}\left[(v_r^n)_{i+\frac{1}{2},j+1} - (v_r^n)_{i+\frac{1}{2},j}\right] + \frac{1}{\delta r}\left[(v_z^n)_{i+1,j+\frac{1}{2}} - (v_z^n)_{i,j+\frac{1}{2}}\right]\right\} \quad (18)$$

2.3 THE SMAC COMPUTING TECHNIQUE

To numerically solve the system defined by Eqs. (3), (4) and (5), subjected to given initial and boundary conditions, a Simplified Marker-and-Cell computing technique (SMAC) is used (Ref. 1). The method considers that the velocity potential of a fluid can be expressed in terms of two potentials $\theta_{i,j}$ and $\psi_{i,j}$, namely

$$\varphi_{i,j} = \theta_{i,j} + \psi_{i,j}/\delta t \qquad \text{(for a full cell)}$$

$$= \psi_{i,j}/\delta t \qquad \text{(for a boundary cell)}$$

$$= \theta_{i,j} \qquad \text{(for a surface cell)}$$

$$= 0 \qquad \text{(for an empty cell).} \qquad (19)$$

The potential $\theta_{i,j}$ is an arbitrary function and may be taken as

$$\theta_{i,j} = g_r r_i + g_z z_i \qquad \text{(for a full cell)}$$

$$= \frac{2\nu}{\delta r}\left[(v_r)_{i+\frac{1}{2},j} - (v_r)_{i-\frac{1}{2},j}\right]$$

(for a surface cell neighboring with only one empty cell, left or right)

$$= \frac{2\nu}{\delta z}\left[(v_z)_{i,j+\frac{1}{2}} - (v_z)_{i,j-\frac{1}{2}}\right]$$

(for a surface cell neighboring with only one empty cell, above or below)

$$= 0 \qquad \text{(otherwise)} . \qquad (20)$$

The potential $\psi_{i,j}$ will be determined such that the velocity potential $\varphi_{i,j}$ will carry a correct value at the completion of each computing cycle. Substituting Eqs. (19) and (20) into Eqs. (13) and (14), one finds

$$(v_r^{n+1})_{i+\frac{1}{2},j} = (\tilde{v}_r^{n+1})_{i+\frac{1}{2},j} - \frac{1}{\delta r}\left[\psi_{i+1,j} - \psi_{i,j}\right] \tag{21}$$

$$(v_z^{n+1})_{i,j+\frac{1}{2}} = (\tilde{v}_r^{n+1})_{i,j+\frac{1}{2}} - \frac{1}{\delta z}\left[\psi_{i,j+1} - \psi_{i,j}\right] \tag{22}$$

where

$$(\tilde{v}_r^{n+1})_{i+\frac{1}{2},j} = (v_r^n)_{i+\frac{1}{2},j} - \delta t \left\{ \frac{1}{r_{i+\frac{1}{2}}\,\delta r}\left[r_{i+1}(v_r^n)^2_{i+1,j} - r_i (v_r^n)^2_{i,j}\right]\right.$$

$$+ \frac{1}{\delta z}\left[(v_r^n v_z^n)_{i+\frac{1}{2},j+\frac{1}{2}} - (v_r^n v_z^n)_{i+\frac{1}{2},j-\frac{1}{2}}\right]$$

$$- \frac{\nu}{(\delta z)^2}\left[(v_r^n)_{i+\frac{1}{2},j+1} + (v_r^n)_{i+\frac{1}{2},j-1} - 2(v_r^n)_{i+\frac{1}{2},j}\right]$$

$$+ \frac{\nu}{\delta r\,\delta z}\left[(v_z^n)_{i+1,j+\frac{1}{2}} - (v_z^n)_{i,j+\frac{1}{2}} - (v_z^n)_{i+1,j-\frac{1}{2}} + (v_z^n)_{i,j-\frac{1}{2}}\right]$$

$$\left. - (f_r^n)_{i,j}\right\} \tag{23}$$

and

$$(\tilde{v}_z^{n+1})_{i,j+\frac{1}{2}} = (v_z^n)_{i,j+\frac{1}{2}} - \delta t \left\{ \frac{1}{r_i \delta r} \left[r_{i+\frac{1}{2}} (v_r^n v_z^n)_{i+\frac{1}{2},j+\frac{1}{2}} - r_{i-\frac{1}{2}} (v_r^n v_z^n)_{i-\frac{1}{2},j+\frac{1}{2}} \right] \right.$$

$$+ \frac{1}{\delta z} \left[(v_z^n)^2_{i,j+1} - (v_z^n)^2_{i,j} \right]$$

$$+ \frac{\nu}{r_i \delta r} \left[r_{i+\frac{1}{2}} \left(\frac{(v_r^n)_{i+\frac{1}{2},j+1} - (v_r^n)_{i+\frac{1}{2},j}}{\delta z} - \frac{(v_z^n)_{i+1,j+\frac{1}{2}} - (v_z^n)_{i,j+\frac{1}{2}}}{\delta r} \right) \right.$$

$$\left. \left. - r_{i-\frac{1}{2}} \left(\frac{(v_r^n)_{i-\frac{1}{2},j+1} - (v_r^n)_{i-\frac{1}{2},j}}{\delta z} - \frac{(v_z^n)_{i,j+\frac{1}{2}} - (v_z^n)_{i-1,j+\frac{1}{2}}}{\delta r} \right) \right] \right.$$

$$\left. - (f_z^n)_{i,j} \right\} \qquad (24)$$

By requiring: (1) the velocities $(\tilde{v}_r^{n+1})_{i+\frac{1}{2},j}$ and $(\tilde{v}_z^{n+1})_{i,j+\frac{1}{2}}$ to satisfy all of the boundary conditions; and (2) the incompressibility property to be fulfilled at the end of each computing cycle (or $D_{i,j}^{n+1} = 0$), the problem reduces to a solution of Poisson's equation with homogeneous boundary conditions, as

$$\frac{1}{r_i (\delta r)^2} \left[r_{i+\frac{1}{2}} (\psi_{i+1,j} - \psi_{i,j}) - r_{i-\frac{1}{2}} (\psi_{i,j} - \psi_{i-1,j}) \right]$$

$$+ \frac{1}{(\delta z)^2}\left[\psi_{i,j+1} - 2\,\psi_{i,j} + \psi_{i,j-1}\right] = \tilde{D}^{n+1}_{i,j} \tag{25}$$

where

$$\tilde{D}^{n+1}_{i,j} = \frac{1}{r_i\,\delta r}\left[r_{i+\frac{1}{2}}(\tilde{v}_r^{n+1})_{i+\frac{1}{2},j} - r_{i-\frac{1}{2}}(\tilde{v}_r^{n+1})_{i-\frac{1}{2},j}\right]$$

$$+ \frac{1}{\delta z}\left[(\tilde{v}_z^{n+1})_{i,j+\frac{1}{2}} - (\tilde{v}_z^{n+1})_{i,j-\frac{1}{2}}\right] \tag{26}$$

Equation (25) is solved by using an iteration process which calculates the value of $\psi^{m+1}_{i,j}$ from the neighboring values of $\psi^{m+1}_{i-1,j}$, $\psi^{m}_{i+1,j}$, $\psi^{m+1}_{i,j-1}$ and $\psi^{m}_{i,j+1}$ until the following condition is satisfied throughout the entire flow field,

$$\left|\frac{|\psi^{m+1}_{i,j}| - |\psi^{m}_{i,j}|}{|\psi^{m+1}_{i,j}| + |\psi^{m}_{i,j}|}\right| < \epsilon_\psi \tag{27}$$

where the superscript m denotes the m^{th} iteration of the n^{th} computing cycle and ϵ_ψ is a constant in the order of 10^{-4}. The formula for calculating $\psi^{m+1}_{i,j}$ is obtained from Eq. (25),

$$\psi^{m+1}_{i,j} = \frac{1}{\frac{2}{(\delta r)^2} + \frac{2}{(\delta z)^2}}\left[\frac{r_{i+\frac{1}{2}}\psi^{m}_{i+1,j} + r_{i-\frac{1}{2}}\psi^{m+1}_{i-1,j}}{r_i(\delta r)^2} + \frac{\psi^{m}_{i,j+1} + \psi^{m+1}_{i,j-1}}{(\delta z)^2} - \tilde{D}^{n+1}_{i,j}\right] \tag{28}$$

After the potential $\psi_{i,j}$ at time $(n+1)\,\delta t$ is found, the appropriate velocity components of the fluid can be readily calculated from Eqs. (21) and (22). The procedure is repeated in the next computing cycle.

Section 3
NUMERICAL SCHEMES

3.1 THE MODIFIED SMAC COMPUTING TECHNIQUE

Most propellant tanks are in the form of cylindrical shells with ellipsoidal ends. Rectangular meshes are not proper in describing the shapes of these tanks, and reducing the mesh size of a problem will drastically increase the solution cost. Hence, other means must be obtained in order to extend the SMAC computing technique to propellant dynamics problems involving curved geometric boundaries.

A method which treats the curved boundary of a fluid as a free surface under a prescribed boundary pressure will be used to study the flow in a container with arbitrary curved boundaries (Ref. 3). The method is to exert a boundary pressure on the free surface such that the normal velocity of the surface vanishes. As shown in Fig. 3, a boundary pressure may be applied to each HS cell, and its magnitude may be determined through an iteration process which relaxes the pressure and velocity fields of the fluid simultaneously. At the completion of a computing cycle, the incompressibility property and all boundary conditions are satisfied, and the existence of a curved boundary is observed in the fluid motion.

To avoid unnecessary computation and complication, a boundary point will be assigned to each HS cell (Fig. 3). The normal velocity of a curved surface will be made to vanish at these points only. Since the potential $\theta_{i,j}$ is an arbitrary known function in the SMAC method, the exerting of a boundary pressure in an HS cell may be stored in $\theta_{i,j}$. The boundary pressure will be varied from one computing cycle to another. Its magnitude may be computed through a continuous adjustment by an amount proportional to the divergence of the velocity (Ref. 3), or

$$\delta\theta/\delta\beta = \overline{V} \cdot \hat{n}/\Delta \qquad (29)$$

where $\delta\beta = \Delta^2/2\delta t$, Δ = minimum of (δr, δz) and $\hat{n}$ is the unit outward normal of a curved surface. It is found that, with a reasonable mesh size, the above scheme performs satisfactorily.

The major steps of a modified SMAC computing cycle are:

Step 1 – Use Eqs. (23) and (24) to compute a set of tentative velocities $\left(\tilde{v}_r^{n+1}\right)_{i+\frac{1}{2}, j}$ and $\left(\tilde{v}_z^{n+1}\right)_{i, j+\frac{1}{2}}$, then calculate $\tilde{D}_{i,j}^{n+1}$ from Eq. (26).

Step 2 – Iterate the $\psi_{i,j}$ field until Eq. (27) is satisfied.

Step 3 – Calculate $\left(v_r^{n+1}\right)_{i+\frac{1}{2}, j}$ and $\left(v_z^{n+1}\right)_{i, j+\frac{1}{2}}$ through Eqs. (21) and (22), and modify these velocities for all boundary and surface cells to satisfy the boundary conditions.

Step 4 – Check the normal velocity of a curved boundary – if its absolute value is sufficiently small to be neglected, Step 5 will be executed; otherwise, the boundary pressure will be adjusted by an amount proportional to $\bar{V} \cdot \hat{n}/\Delta$ and Steps 1 through 4 will be repeated.

Step 5 – Displace the marker particles according to their local velocities.

Step 6 – Modify the velocities of all boundary and surface cells to satisfy the boundary conditions of the newly obtained flow field.

The numerical stability of the modified SMAC computing technique was investigated. If the time increment δt and the iteration step $\delta\beta$ are chosen to satisfy the following two inequalities

$$2\nu\ \delta t < \frac{(\delta r)^2 (\delta z)^2}{(\delta r)^2 + (\delta z)^2} \tag{30}$$

and

$$\delta\beta \leq \frac{\delta r\, \delta z}{2\, \delta t}\ , \tag{31}$$

a covergent solution may be obtained. Also, the execution time of a simulation run is found to be dependent on the mesh size and tank geometry but not on the material properties of a fluid. These criteria are not necessarily always true, however, and apparently do not apply to surface instabilities of low viscosity fluids as discussed in Section 6.

The dynamic loads exerted by a moving liquid on its container may be expressed by the surface integrals

$$\overline{F} = \int_S p\,\hat{n}\,ds$$

and

$$\overline{M} = \int_S p\,\overline{r} \times \hat{n}\,dS,$$

where $\overline{F}$ and $\overline{M}$ are the total force and moment exerted by a liquid on the container, respectively, and $\overline{r}$ is a position vector. In a MAC formulation, the integrals are evaluated by summing up the quantities contributed by all cells neighboring with or falling on the container wall. The loads may be calculated at the end of one or several computing cycles. If these loads are plotted against time, the data points may be scattered and smooth curves may be drawn to give the best fit.

3.2 BOUNDARY CONDITIONS

The treatment of the pressure in a boundary cell has been discussed in Sections 2.3 and 3.1 (through $\theta_{i,j}$ and $\psi_{i,j}$). The velocities of a boundary cell are computed by satisfying the incompressibility property and the boundary conditions of the fluid. Using Eqs. (11), (12) and (15) through (18), the velocities of various boundary cells may be defined as follows:

1. Boundary velocities of a B cell

   As shown in Fig. 4, the velocities of a B cell may be computed to satisfy the conditions of a rigid smooth wall.

2. Boundary velocities of an S or HS cell

   The velocities of an S or HS cell are computed to satisfy the incompressibility property and the conditions of a free surface. There are 15 possible arrangements of E and HE cells around an S or HS cell. Fig. 5 shows the possible arrangements and Table 1 lists the appropriate equations for calculating the velocities.

Table 1

EQUATIONS FOR CALCULATING THE VELOCITIES OF AN S OR HS CELL

Configuration (See Fig. 5)	Equations to be Used
1, 5, 11, 13, 15	Eq. (32)
2, 7, 10, 14	Eq. (33)
3	Eqs. (34) and (37)
4	Eq. (35)
6	Eqs. (36) and (37)
8	Eq. (38)
9	Eqs. (34) and (39)
12	Eqs. (36) and (39)

Equations (32) through (39) are:

$$(v_r)_{i+\frac{1}{2},j} = \frac{1}{r_{i+\frac{1}{2}}}\left\{r_{i-\frac{1}{2}}(v_r)_{i-\frac{1}{2},j} - \frac{r_i\,\delta r}{\delta z}\left[(v_z)_{i,j+\frac{1}{2}} - (v_z)_{i,j-\frac{1}{2}}\right]\right\} \quad (32)$$

$$(v_z)_{i,j+\frac{1}{2}} = (v_z)_{i,j-\frac{1}{2}} - \frac{\delta z}{r_i\,\delta r}\left[r_{i+\frac{1}{2}}(v_r)_{i+\frac{1}{2},j} - r_{i-\frac{1}{2}}(v_r)_{i-\frac{1}{2},j}\right] \quad (33)$$

$$(v_r)_{i+\frac{1}{2},j} = \frac{4\,r_i - \delta z}{4\,r_i + \delta r}(v_r)_{i-\frac{1}{2},j} \quad (34)$$

$$(v_r)_{i-\frac{1}{2},j} = \frac{1}{r_{i-\frac{1}{2}}}\left\{r_{i+\frac{1}{2}}(v_r)_{i+\frac{1}{2},j} + \frac{r_i\,\delta r}{\delta z}\left[(v_z)_{i,j+\frac{1}{2}} - (v_z)_{i,j-\frac{1}{2}}\right]\right\} \quad (35)$$

$$(v_r)_{i-\frac{1}{2},j} = \frac{4\,r_i + \delta r}{4\,r_i - \delta r}\,(v_r)_{i+\frac{1}{2},j} \tag{36}$$

$$(v_z)_{i,j+\frac{1}{2}} = (v_z)_{i,j-\frac{1}{2}} - \frac{\delta z}{4\,r_i}\left[(v_r)_{i+\frac{1}{2},j} + (v_r)_{i-\frac{1}{2},j}\right]$$

$$= (v_z)_{i,j-\frac{1}{2}} \qquad \text{(in case of planar flow)} \tag{37}$$

$$(v_z)_{i,j-\frac{1}{2}} = (v_z)_{i,j+\frac{1}{2}} + \frac{\delta z}{r_i\,\delta r}\left[r_{i+\frac{1}{2}}\,(v_r)_{i+\frac{1}{2},j} - r_{i-\frac{1}{2}}\,(v_r)_{i-\frac{1}{2},j}\right] \tag{38}$$

$$(v_z)_{i,j-\frac{1}{2}} = (v_z)_{i,j+\frac{1}{2}} + \frac{\delta z}{4\,r_i}\left[(v_r)_{i+\frac{1}{2},j} + (v_r)_{i-\frac{1}{2},j}\right]$$

$$= (v_z)_{i,j+\frac{1}{2}} \qquad \text{(in case of planar flow)} \tag{39}$$

3. <u>Boundary velocity between two neighboring E and/or HE cells just outside a free surface</u>

The velocity between two neighboring empty cells just outside a free surface is computed in a way of satisfying the free stress conditions. There are four possible cases where the velocities need to be adjusted (see Fig. 6):

<u>Case 1</u> $$(v_z)_{i+1,j+\frac{1}{2}} = (v_z)_{i,j+\frac{1}{2}} - \frac{\delta r}{\delta z}\left[(v_r)_{i+\frac{1}{2},j+1} - (v_r)_{i+\frac{1}{2},j}\right] \tag{40}$$

<u>Case 2</u> $$(v_r)_{i+\frac{1}{2},j+1} = (v_r)_{i+\frac{1}{2},j} - \frac{\delta z}{\delta r}\left[(v_z)_{i+1,j+\frac{1}{2}} - (v_z)_{i,j+\frac{1}{2}}\right] \tag{41}$$

<u>Case 3</u> $$(v_z)_{i-1,j+\frac{1}{2}} = (v_z)_{i,j+\frac{1}{2}} + \frac{\delta r}{\delta z}\left[(v_r)_{i-\frac{1}{2},j+\frac{1}{2}} - (v_r)_{i-\frac{1}{2},j}\right] \tag{42}$$

$$\underline{\text{Case 4}} \quad (v_r)_{i+\frac{1}{2},\,j-1} = (v_r)_{i+\frac{1}{2},\,j} + \frac{\delta z}{\delta r}\left[(v_z)_{i+1,\,j-\frac{1}{2}} - (v_z)_{i,\,j-\frac{1}{2}}\right] \qquad (43)$$

3.3 SURFACE TENSION EFFECTS

The surface tension of a liquid plays an important role in zero-g hydrostatics and propellant reorientation. Its influence in a transient flow will depend on the body and inertia forces of the liquid (Ref. 6). To study the surface tension effects in propellant dynamics, a method of including surface tension in the marker-and-cell computing technique (Ref. 4) was programmed and incorporated into the modified SMAC computer program (LHMAC2). A 7th order least squares curve fitting routine (a library routine of MSFC's Univac 1108 computer system) is used to find an approximate free surface from the surface marker particles whenever the surface tension force is needed. The free surface is restricted to a smooth simple surface and the LHMAC2 program will automatically divide the surface into segments expressed by polynomials, as

$$z = \sum_{i=0}^{7} a_i\, r^i \qquad \text{(for segments 1 or 3)} \qquad (44)$$

or

$$r = \sum_{i=0}^{7} b_i\, z^i \qquad \text{(for segments 2 or 4)} \qquad (45)$$

where a_i and b_i are the least square coefficients (Fig. 7). Using Eqs. (44) and (45), the principal curvatures of a free surface can be readily computed, and the surface tension forces may be obtained from the following equations:

$$\left\{\begin{array}{l} f_r = -\dfrac{\tau}{\rho}\left\{\dfrac{z'z''}{\left[1+(z')^2\right]^2} + \dfrac{(z')^2}{r\left[1+(z')^2\right]}\right\} \\ f_z = \dfrac{\tau}{\rho}\left\{\dfrac{z''}{\left[1+(z')^2\right]^2} + \dfrac{z'}{r\left[1+(z')^2\right]}\right\} \end{array}\right. \qquad \text{(for segments 1 or 3)} \qquad (46)$$

or

$$\begin{cases} f_r = \dfrac{\tau}{\rho}\left\{\dfrac{r''}{\left[1+(r')^2\right]^2} - \dfrac{1}{r\left[1+(r')^2\right]}\right\} \\ \\ f_z = \dfrac{\tau}{\rho}\left\{\dfrac{-r'\,r''}{\left[1+(r')^2\right]^2} + \dfrac{r'}{r\left[1+(r')^2\right]}\right\} \end{cases} \quad \text{(for segments 2 or 4)} \quad (47)$$

where τ is the surface tension coefficient of a liquid (Refs. 2, 4, and 5). In a rectangular mesh, these forces are applied at the boundaries of an S cell. Similarly, the corresponding equations for planar flow are:

$$y = \sum_{i=0}^{7} a_i x^i \qquad \text{(for segments 1 or 3);} \quad (48)$$

$$x = \sum_{i=0}^{7} b_i y^i \qquad \text{(for segments 2 or 4);} \quad (49)$$

$$\begin{cases} f_x = -\dfrac{\tau}{\rho}\dfrac{y'\,y''}{\left[1+(y')^2\right]^2} \\ \\ f_y = \dfrac{\tau}{\rho}\dfrac{y''}{\left[1+(y')^2\right]^2} \end{cases} \qquad \text{(for segments 1 or 3);} \quad (50)$$

and

$$\begin{cases} f_x = \dfrac{\tau}{\rho} \dfrac{x''}{\left[1 + (x')^2\right]^2} \\ \\ f_y = -\dfrac{\tau}{\rho} \dfrac{x' x''}{\left[1 + (x')^2\right]^2} \end{cases} \quad \text{(for segments 2 or 4).} \qquad (51)$$

Section 4
THE COMPUTER PROGRAM

A modified SMAC computer program (LHMAC2) for studying propellant dynamics problems was developed. The program is written in FORTRAN V language and requires a 55 K storage capacity. The LHMAC2 program can be used to simulate the flow in an axisymmetric or a channel-type container requiring up to 1200 cells. The output of the program will provide the following data which are pertinent to propellant dynamics:

- Plots of the marker particle and velocity fields of a transient flow;
- Pressure distribution along a container wall; and
- Forces and moments induced by a moving liquid in a closed container.

Continued improvement of the LHMAC2 program is planned and additional problems on propellant dynamics will be simulated. A brief block diagram which shows the program organization of the LHMAC2 program is given in Chart 1.

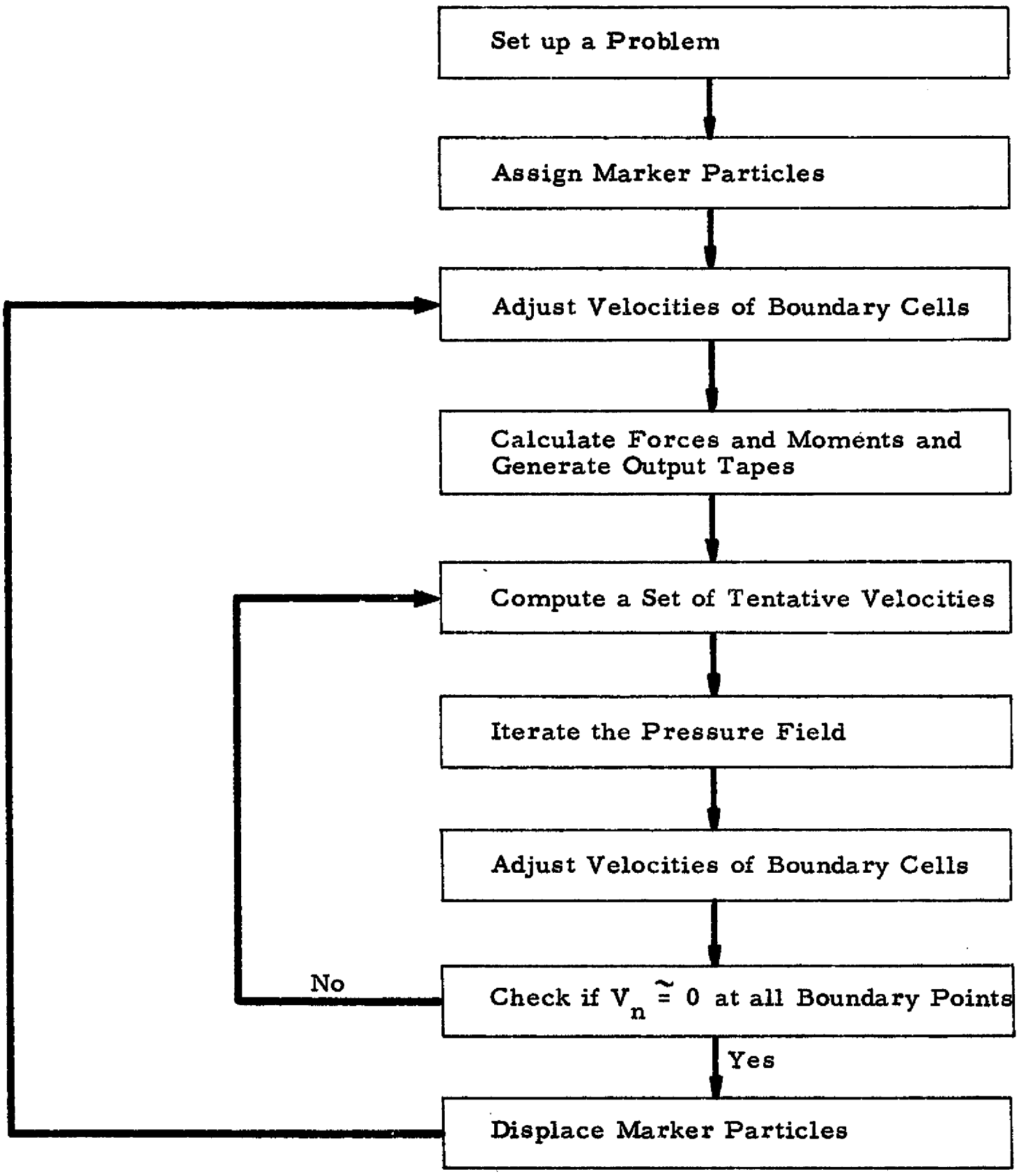

Chart 1 - Program Organization of the LHMAC2 Program

Section 5
EXAMPLES

Three types of problems which may be encountered in propellant dynamics are investigated:

- Vehicle separation;
- Engine restart; and
- Docking slosh.

The impact force transmitted to a container is simulated through an equivalent gravitational acceleration. The dynamic aspects of these problems are indicated by the forces and moments exerted by the liquid propellant on the container. Also, plots of the flow and velocity fields of the propellant are provided as a visual presentation.

The mesh size, tank geometry, equivalent gravitational acceleration and kinematic viscosity coefficient are considered as the main parameters of a problem. Examples of the three types of problems which were investigated in this study are given below:

Example 1: The flow of a liquid propellant in a channel-type container is used to estimate the forces and moments exerted by the propellant on a booster tank during the separation of the orbiter and booster. Tank geometry and propellant level of the problem are shown in Fig. 8, and important parameters for the simulation are,

$$g_x = 6.0 \text{ m/sec}^2 \quad (t \leq 0.7 \text{ sec})$$
$$= 0.0 \quad (t > 0.7 \text{ sec})$$
$$g_y = 0.0$$
$$\nu = 1.7 \times 10^{-7} \text{ m}^2/\text{sec}$$

$$\rho = 1140.0 \text{ kg/m}^3$$

$$\delta t = 0.05 \text{ sec}$$

$$\delta\beta = 2.0 \text{ m}^2/\text{sec}$$

The flow and velocity fields of propellant at selected times are shown in Figs. 9, 10, 11 and 12. The pressure distributions along the tank wall at t = 0.6 and 0.8 sec are given in Fig. 13. The forces and moments exerted by the propellant on the container are shown in Fig. 14.

Example 2: The flow of a liquid propellant in an axisymmetric tank during engine restart is simulated by using the parameters listed in Table 2. This example shows how a viscous transient flow can be influenced by the equivalent gravitational acceleration and the kinematic viscosity coefficient. The propellant is assumed to be under a low-g condition initially, and its static free surface is taken as

$$\left(\frac{r}{3.6}\right)^2 + \left(\frac{z-3.6}{2.1}\right)^2 = 1$$

Figure 15 shows the tank geometry and propellant level of the problem. The flow and velocity fields of all cases at selected times are given in Figs. 16 through 25.

Table 2
PARAMETERS USED IN THE VARIOUS CASES OF EXAMPLE 2

Case	A	B	C
g_r (m/sec^2)	0.0	0.0	0.0
g_z (m/sec^2)	-1.0	-5.0	-1.0
ν (m^2/sec)	1.7×10^{-7}	1.7×10^{-7}	0.5
ρ (kg/m^3)	1140.0	1140.0	1140.0
δt (sec)	0.025	0.025	0.025
$\delta\beta$ (m^2/sec)	1.75	1.75	1.75

Example 3: Using LHMAC2 program, the flow of a liquid propellant during a docking maneuver is simulated through the following two sample problems:

Sample Problem I (Axisymmetric Tank)	Sample Problem II (Channel-Type Tank)
$g_r = 0.0$	$g_x = 0.1$ m/sec^2
$g_z = 1.0$ m/sec^2	$g_y = 1.0$ m/sec^2
$\nu = 0.5$ m^2/sec	$\nu = 0.5$ m^2/sec
$\rho = 1.0$ kg/m^3	$\rho = 1.0$ kg/m^3
$\delta t = 0.05$ sec	$\delta t = 0.05$ sec
$\delta\beta = 2.0$ m^2/sec	$\delta\beta = 2.0$ m^2/sec

The tank geometries and propellant levels of these problems are shown in Figs. 26 and 27. The flow and velocity fields of the problems are given in Figs. 28 - 32. To show the dynamic aspect of the moving liquid, the forces and moments exerted by the liquid on the container are computed (see Figs. 33, 34 and 35). Note that N and N-m per unit width are used as the units of the forces and moments exerted on a channel-type tank, respectively.

Section 6
CONCLUSIONS AND RECOMMENDATIONS

Based on the Marker-and-Cell (MAC) computing technique, a two-dimensional computer program (LHMAC2) was developed. Using the LHMAC2 program, the flow of a liquid propellant in axisymmetric or channel-type tanks during various space maneuvers was simulated and encouraging results were obtained. From this study, it is found that the MAC method can be used to study the problems in propellant dynamics, and the method has a great potential to be extended to three-dimensional problems. Furthermore, due to the lack of solutions to problems of engineering interest, an effort should be made to develop a three-dimensional MAC computer program.

The kinematic viscosity coefficient of a liquid has a strong influence on the calculated free surface and flow speed (see Examples 1, 2 and 3). In general, a liquid (such as cryogenic propellant or water) with a kinematic viscosity coefficient of the order of 10^{-7} m^2/sec will have a wavy, unstable free surface. Unfortunately, no reference was found which discussed this phenomenon. The present numerical schemes of the modified SMAC program can be refined to eliminate some of these instabilities. Experimental confirmation is needed, however, before a meaningful improvement can be made.

The surface tension effect of a liquid is included in this study. The influence of surface tension in a transient flow was investigated. For flows under an equivalent gravitational acceleration of the order of 10^{-2} g_o or higher, no significant influence due to the inclusion of surface tension was observed (note that $g_o \simeq 9.8$ m/sec^2).

REFERENCES

1. Amsden, A.A., and F.H. Harlow, "The SMAC Method: A Numerical Technique for Calculating Incompressible Fluid Flows," LA-4370, Los Alamos Scientific Laboratory of the University of California, Los Alamos, N.M., May 1970.

2. Welch, J.E., F.H. Harlow, J.P. Shannon and B.J. Daly, "The MAC Method: A Computing Technique for Solving Viscous, Incompressible, Transient Fluid-Flow Problems Involving Free Surface," LA-3425, Los Alamos Scientific Laboratory of the University of California, Los Alamos, N.M., January 1969.

3. Viecelli, J.A., "A Method for Including Arbitrary External Boundaries in the MAC Incompressible Fluid Computing Technique," J. of Comp. Phys., Vol. 4, 1969, pp. 543-551.

4. Daly, B.J., "A Technique for Including Surface Tension Effects in Hydrodynamics Calculations," J. of Comp. Phys., Vol. 4, 1969, pp. 97-117.

5. "Engineering Data Section," Cryogenic Engineering, Vol. 3, No. 1., 1968, pp. 81-108.

6. Abramson, H. N., Ed., "The Dynamic Behavior of Liquids in Moving Containers," NASA SP-106, National Aeronautics and Space Administration, Washington, D.C., 1966.

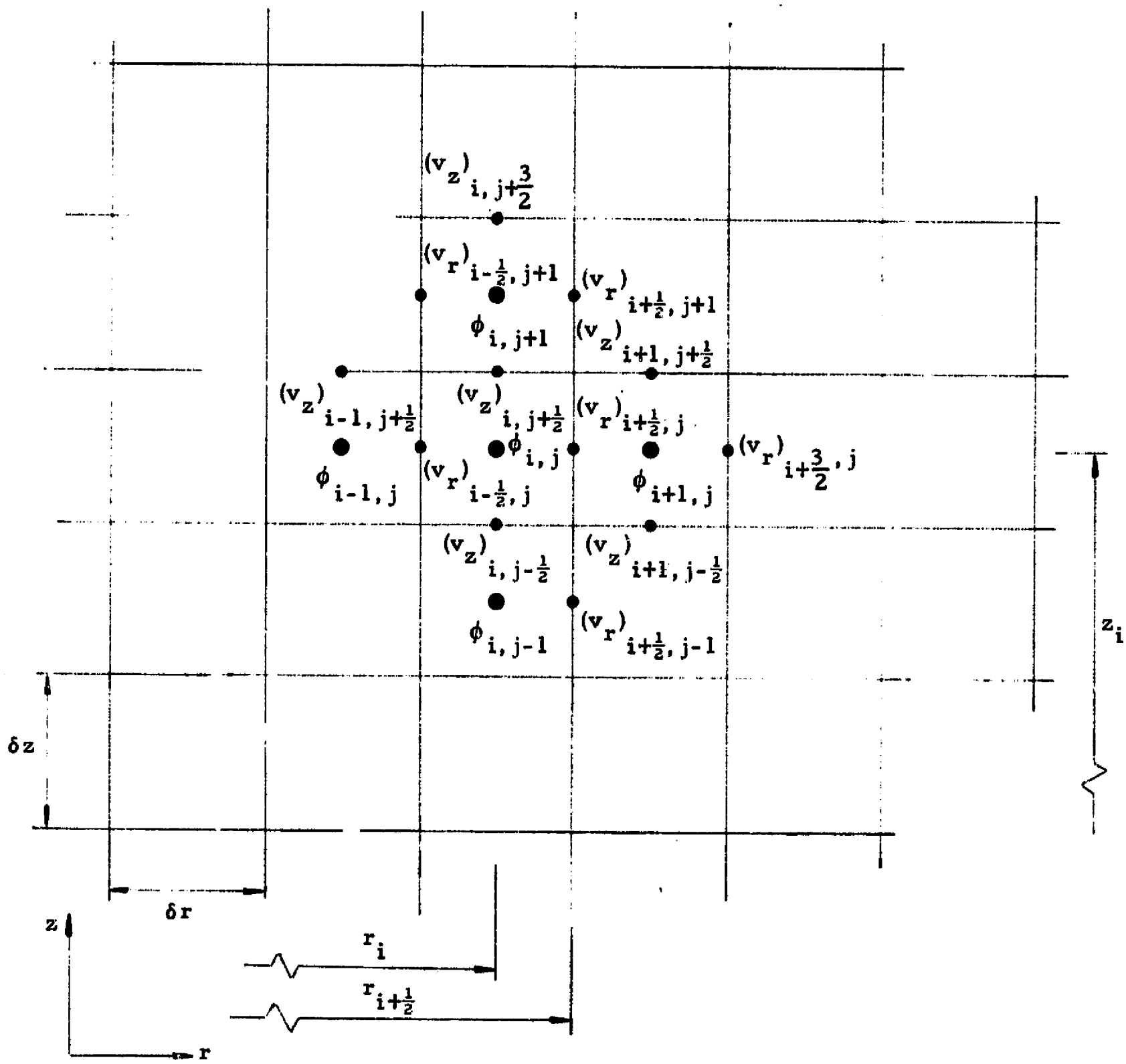

Fig. 1 - Velocities and Velocity Potential in a Rectangular Mesh

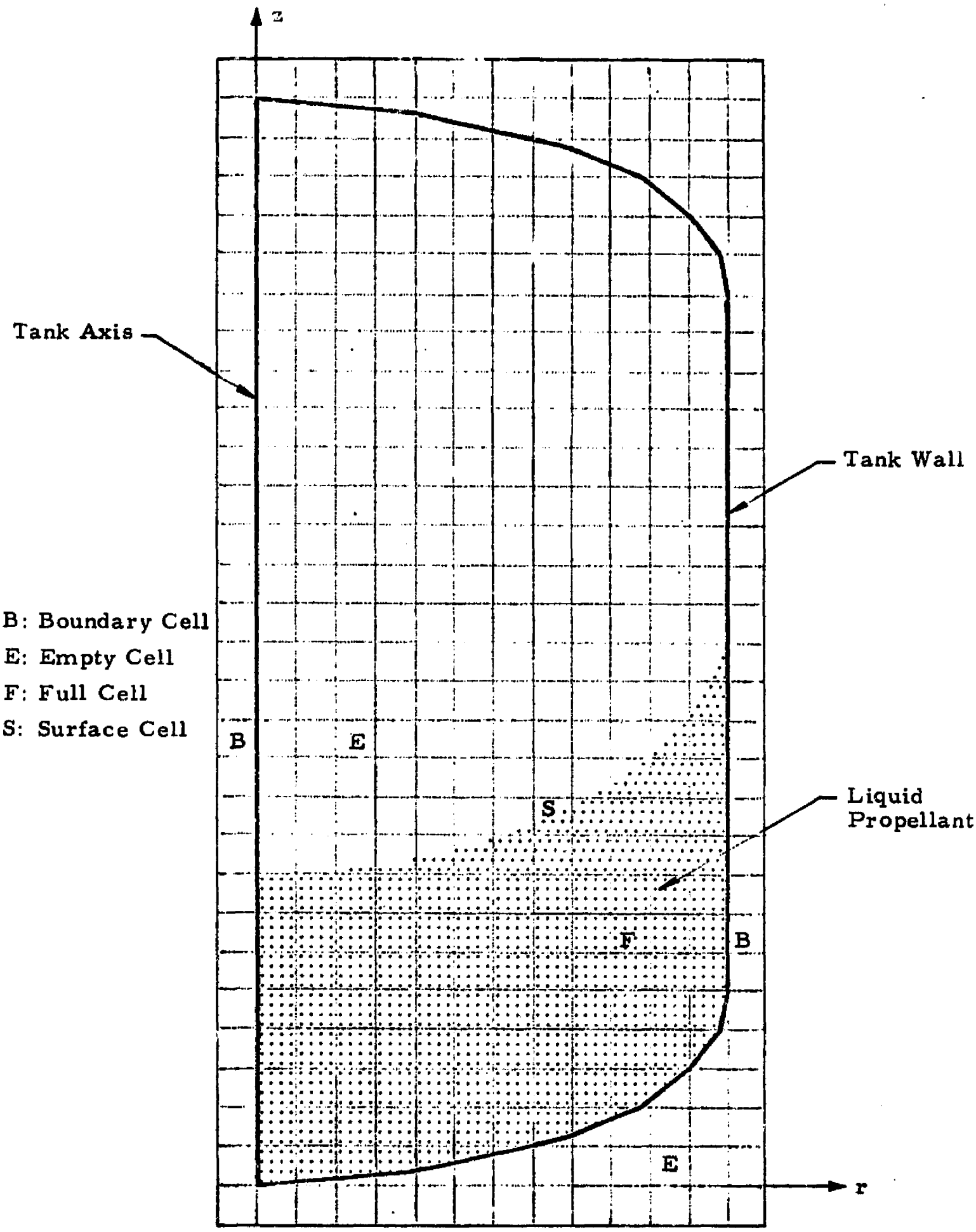

Fig. 2 - Possible Cell Status in a Computing Cycle

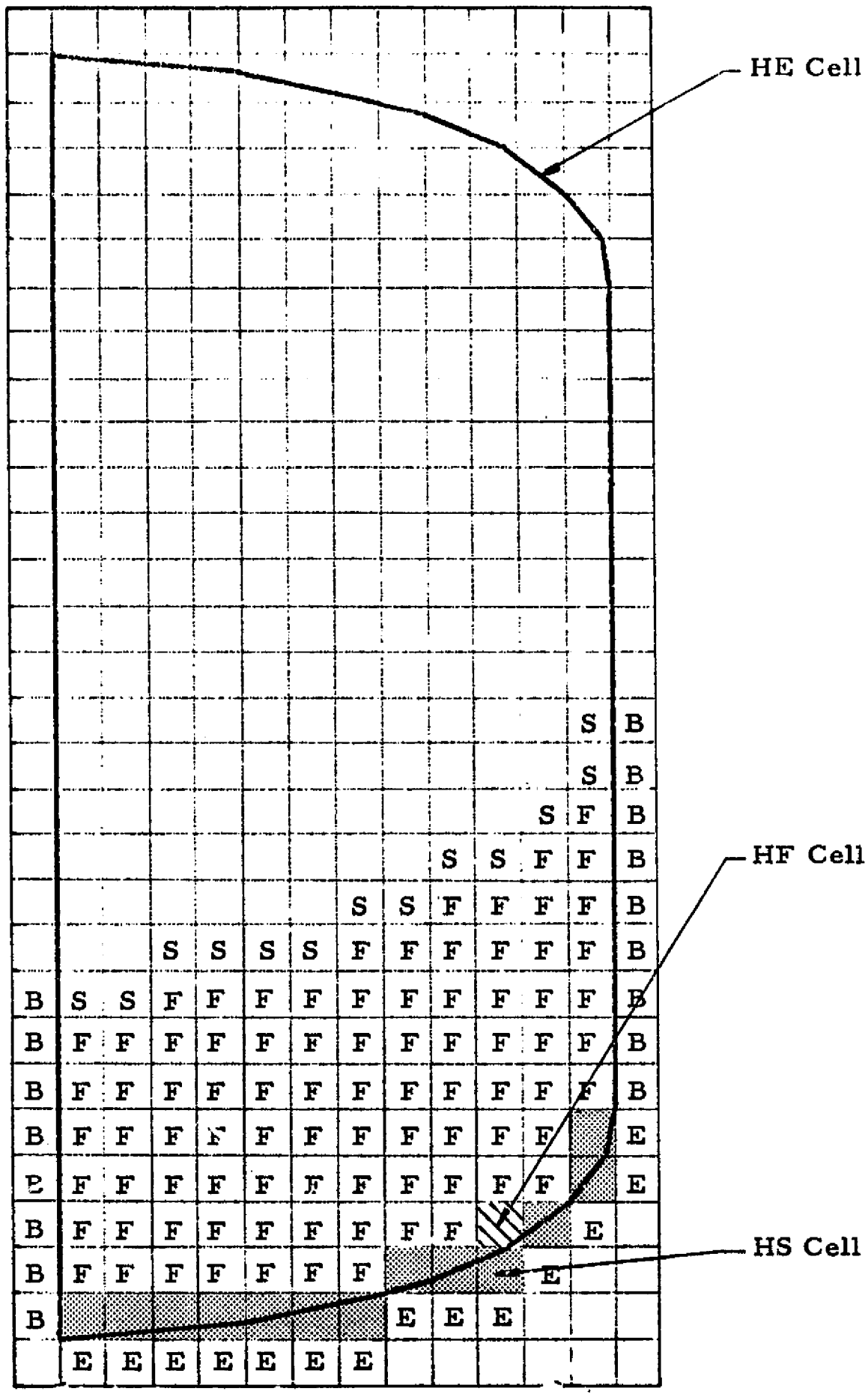

Fig. 2 (Continued)

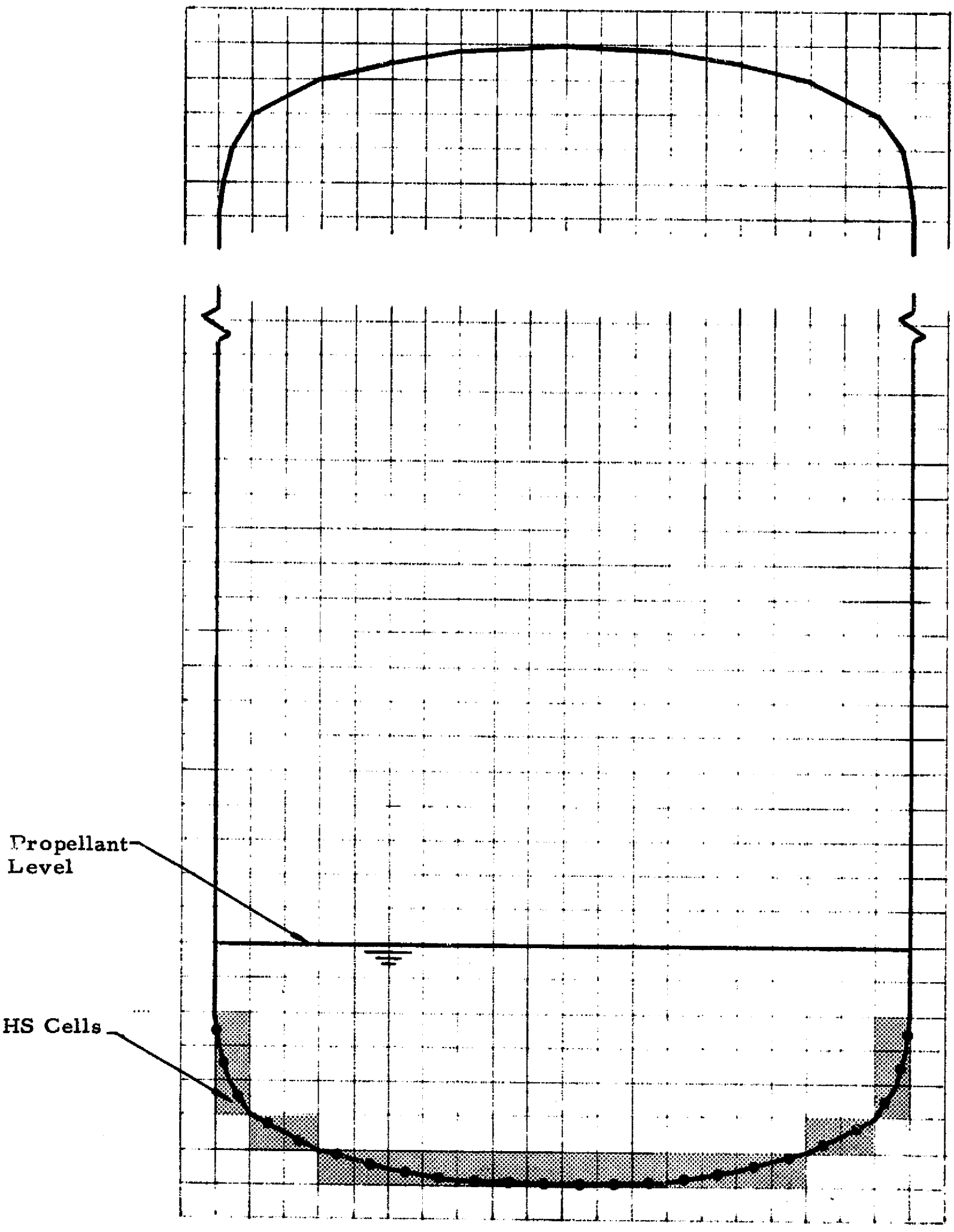

Fig. 3 - Assignment of Boundary Points Along a Curved Boundary

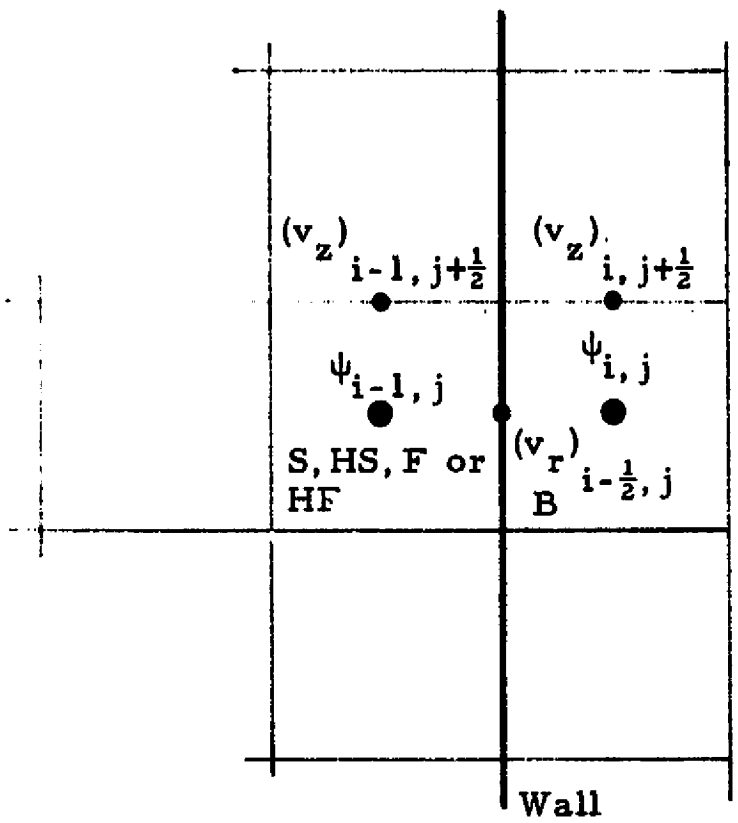

$(v_r)_{i-\frac{1}{2}, j} = 0$

$(v_z)_{i, j+\frac{1}{2}} = (v_z)_{i-1, j+\frac{1}{2}}$

$\psi_{i, j} = \psi_{i-1, j}$

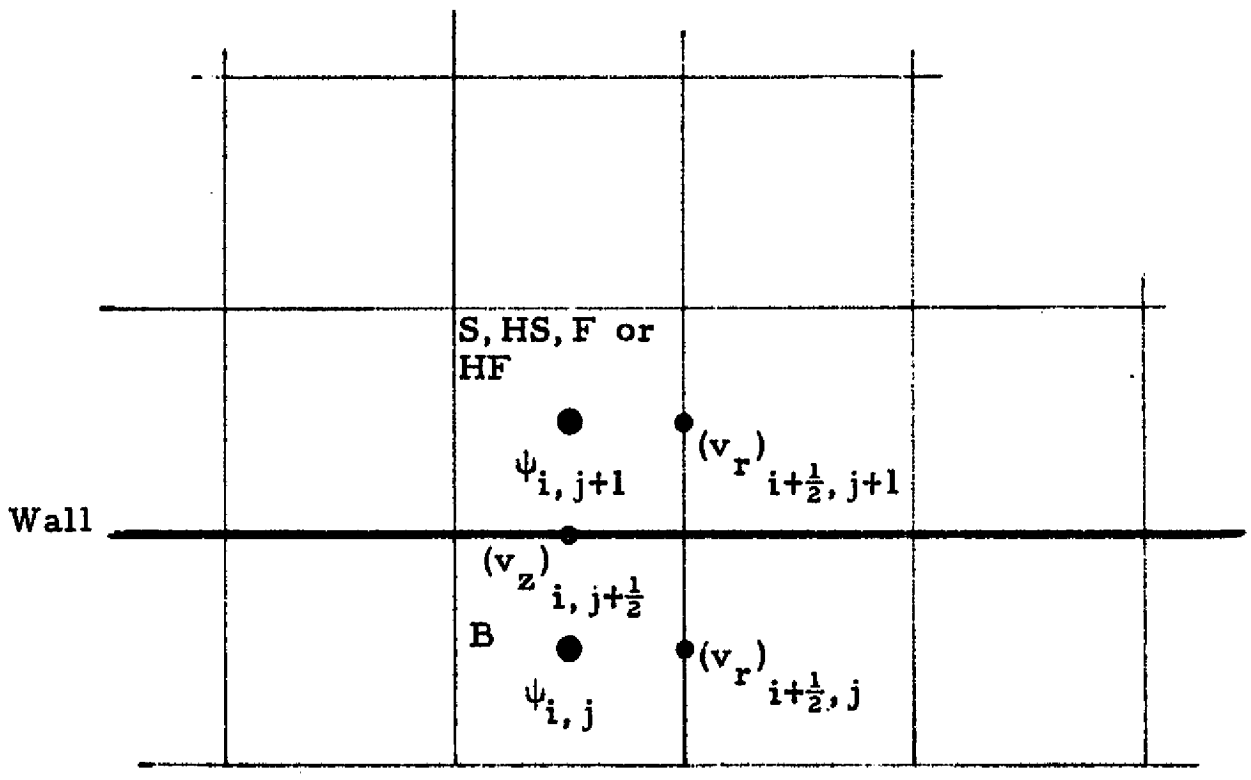

$(v_r)_{i+\frac{1}{2}, j} = (v_r)_{i+\frac{1}{2}, j+1}$, $(v_z)_{i, j+\frac{1}{2}} = 0$, $\psi_{i, j} = \psi_{i, j+1}$

Fig. 4 - Boundary Values of a B Cell

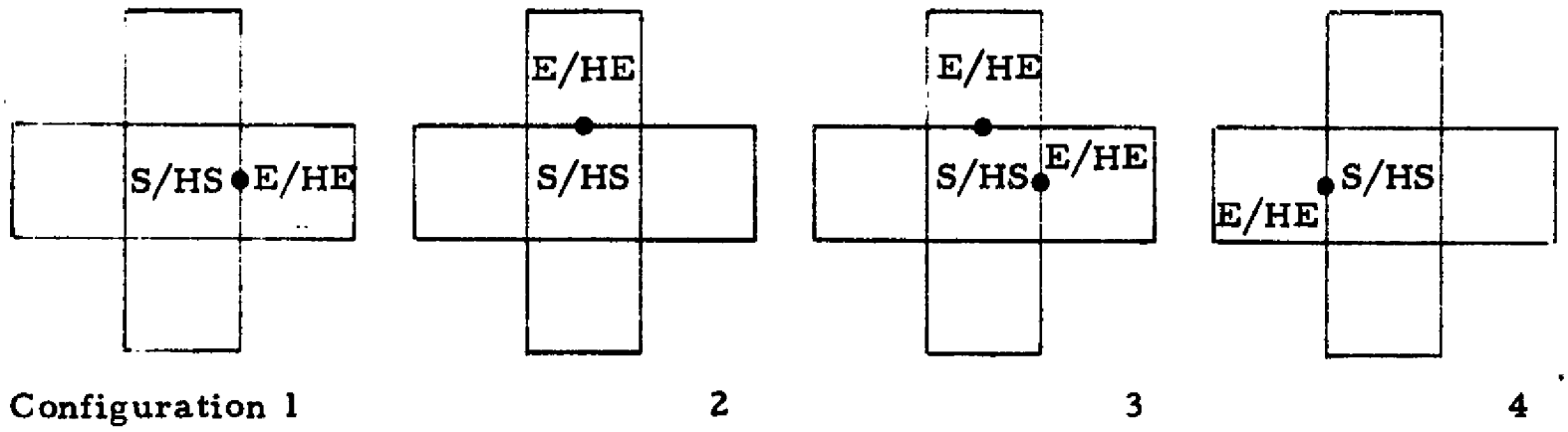

Fig. 5 - Fifteen Possible Arrangements of E and HE Cells Around an S or HS Cell

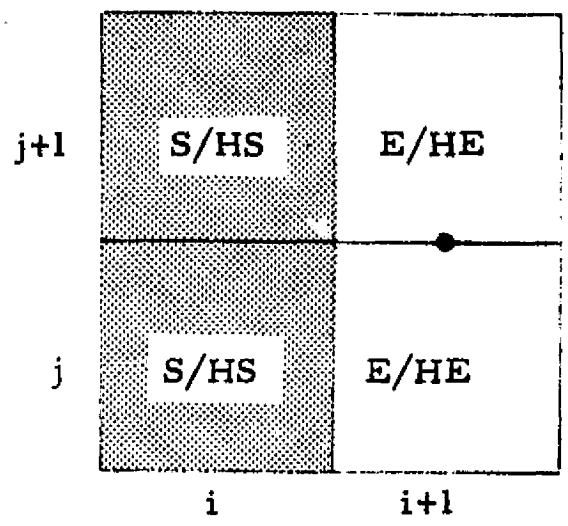

Case 1

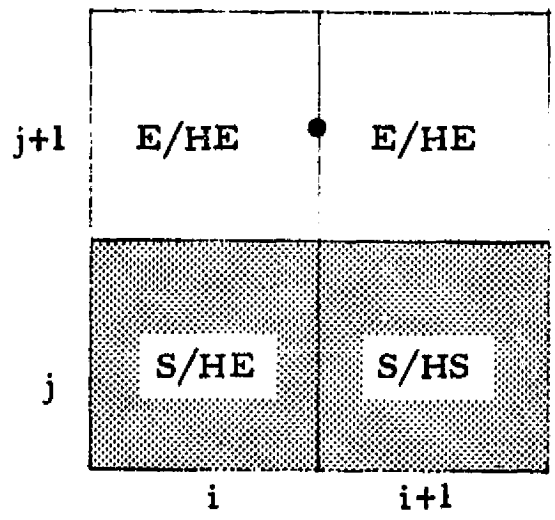

Case 2

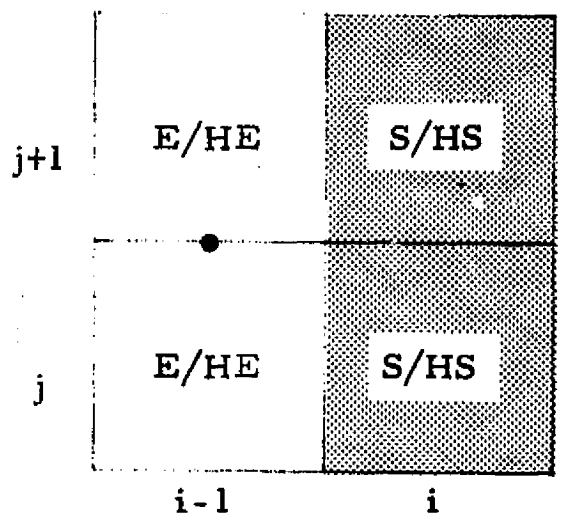

Case 3

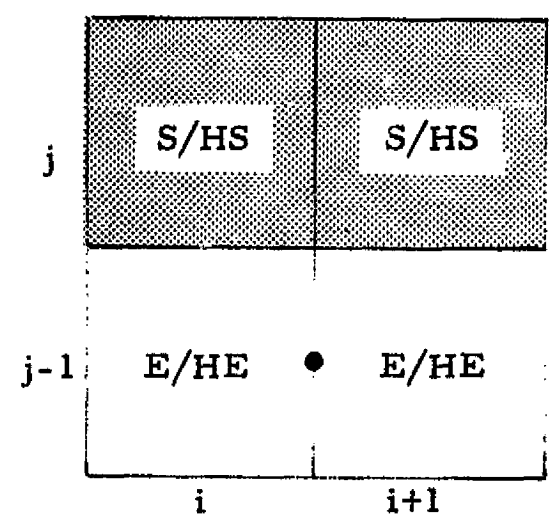

Case 4

Fig. 6 - Four Possible Cases of Empty Cells Having Non-Zero Velocities

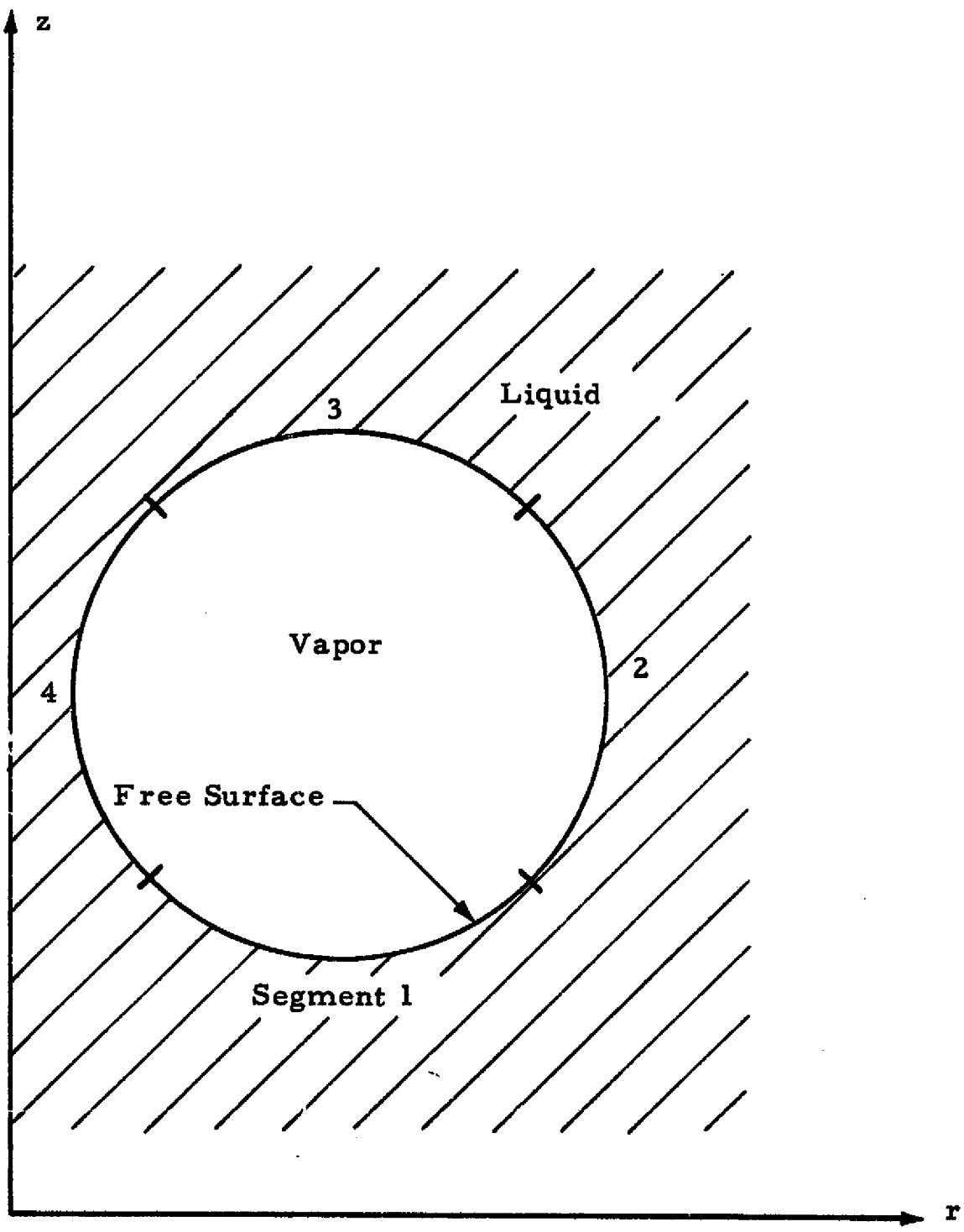

Fig. 7 - Free Surface of a Liquid

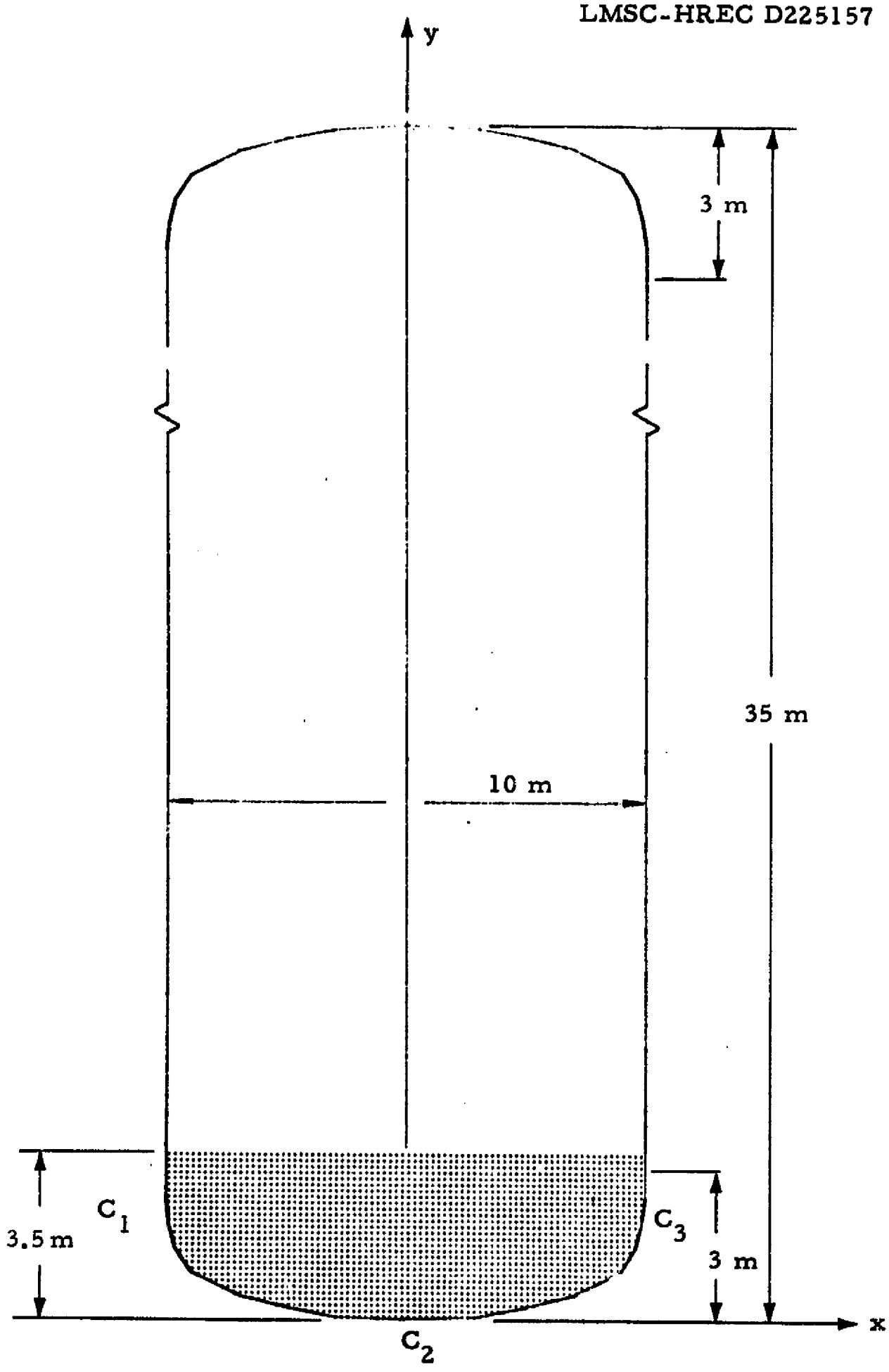

Example 1

Fig. 8 - Tank Geometry and Propellant Level

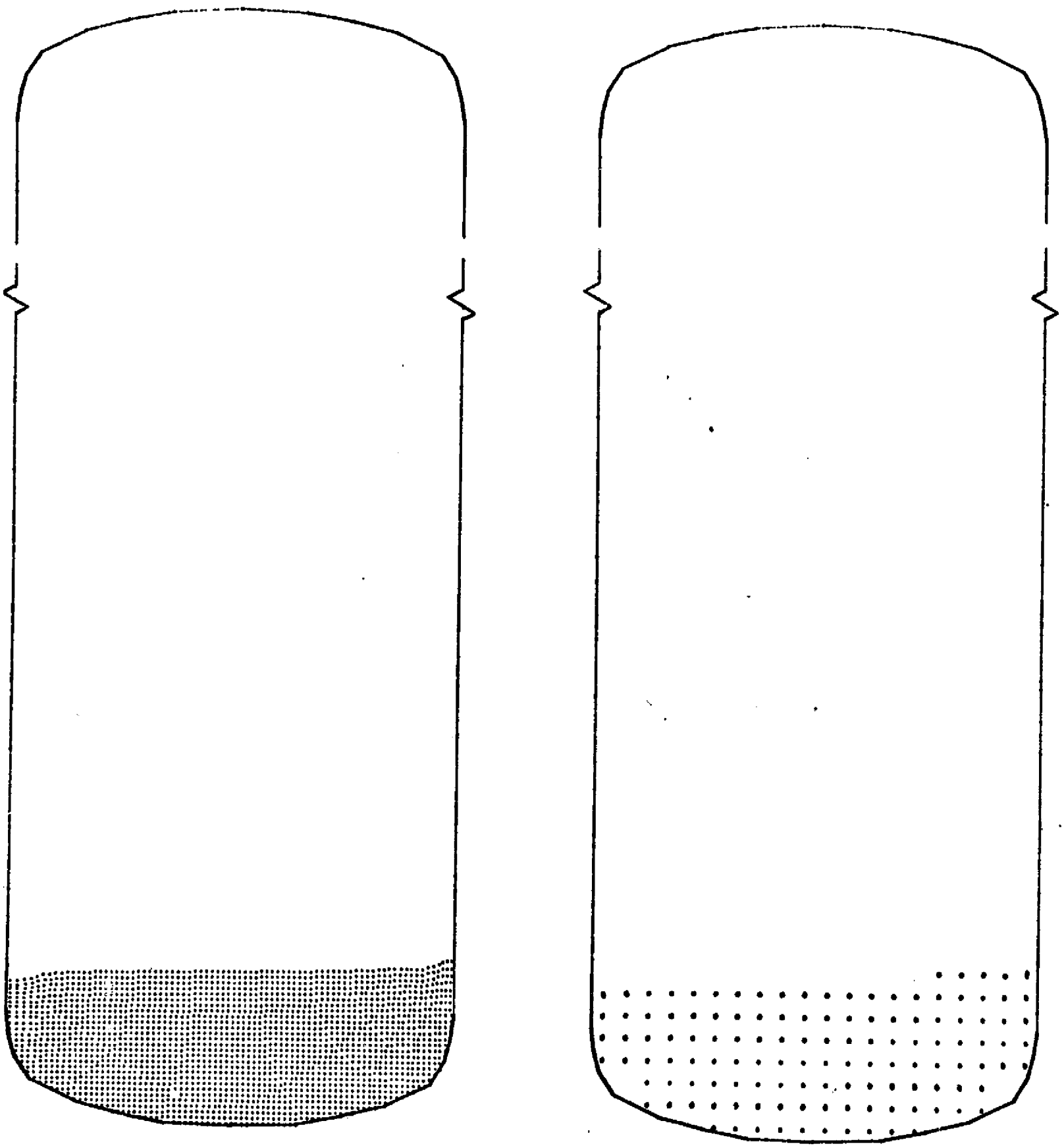

Example 1

Fig. 9 - Flow and Velocity Fields at t = 0.2 sec.

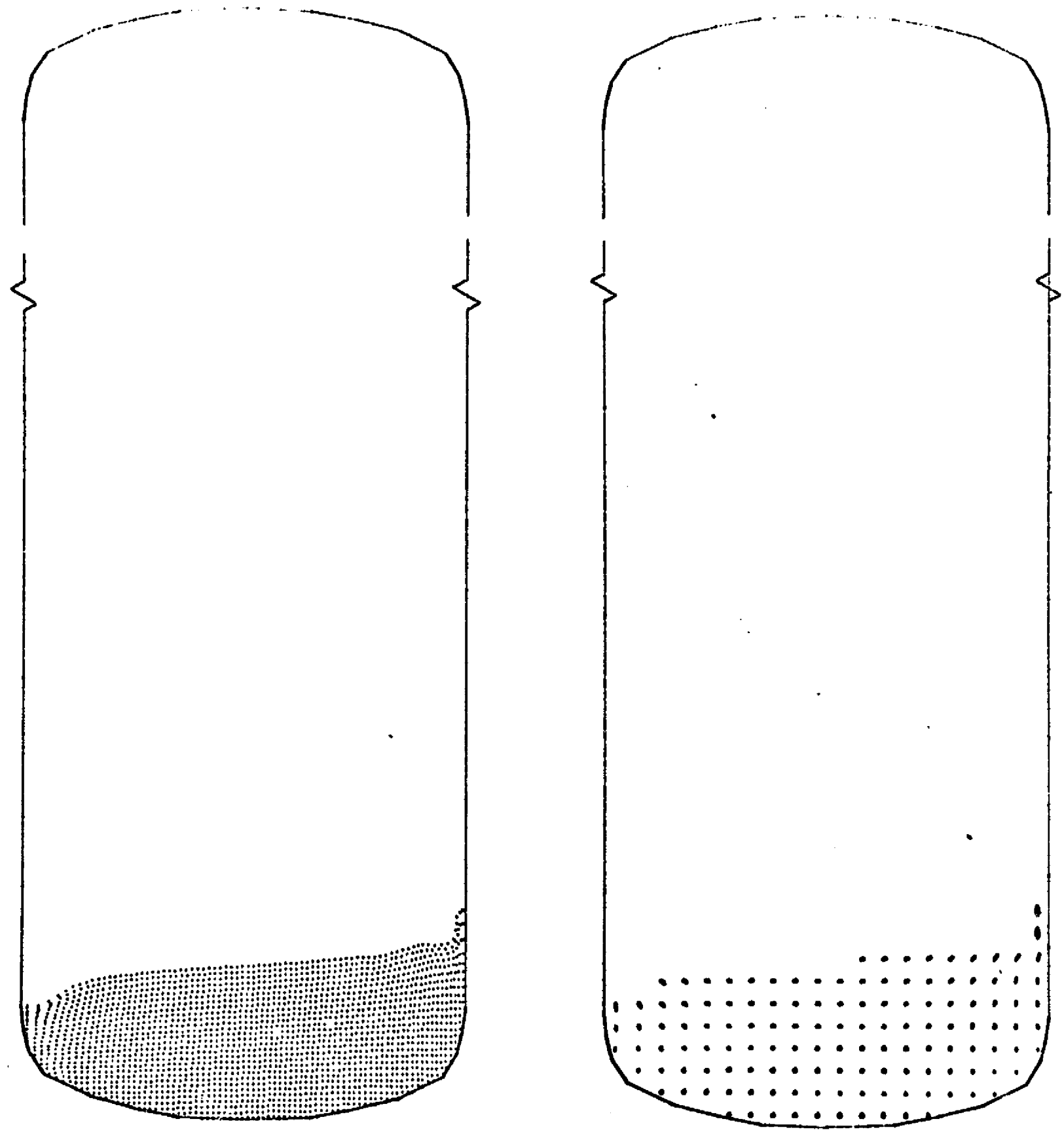

Example 1

Fig. 10 - Flow and Velocity Fields at t = 0.4 sec

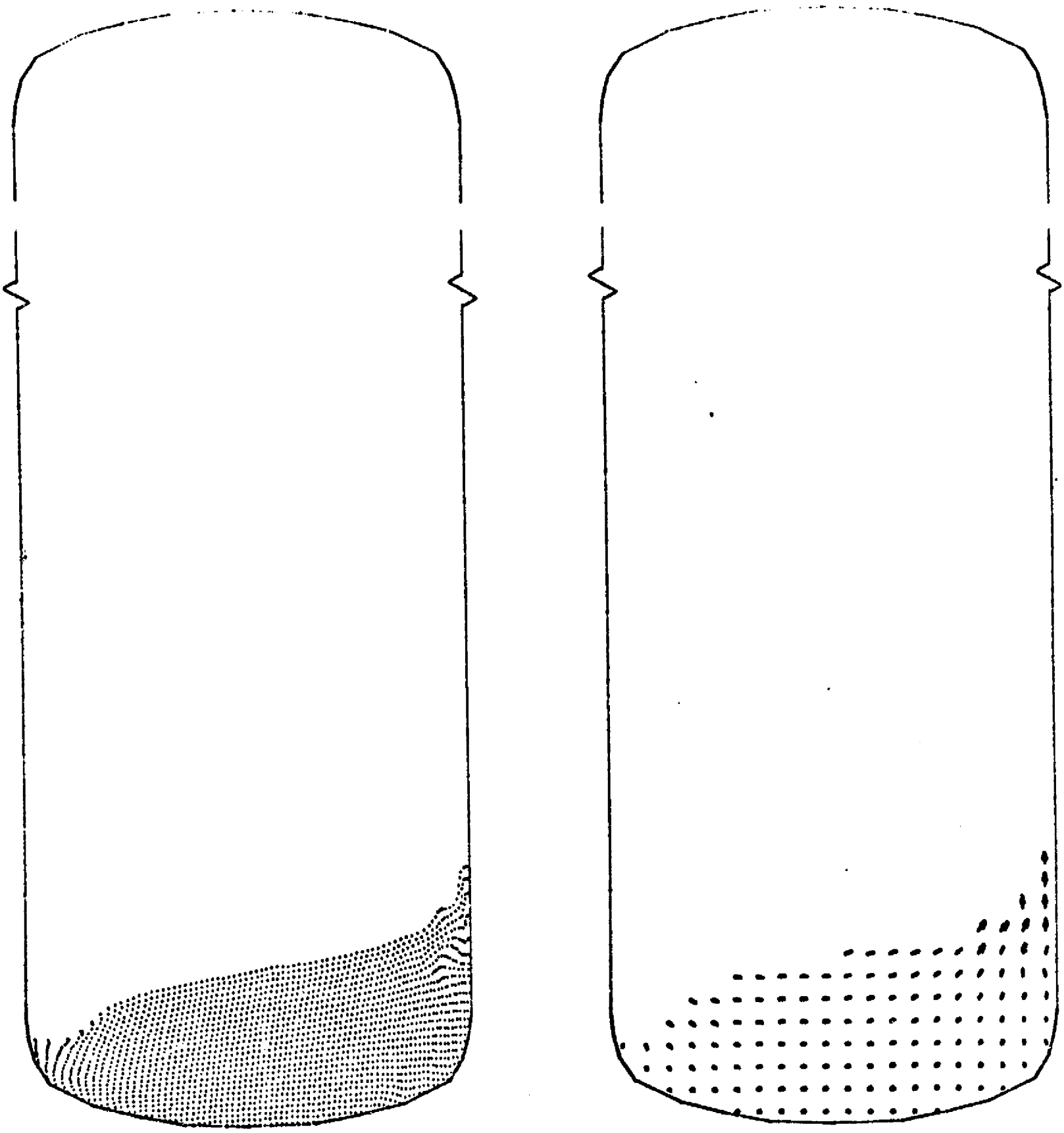

Example 1

Fig. 11 - Flow and Velocity Fields at t = 0.6 sec

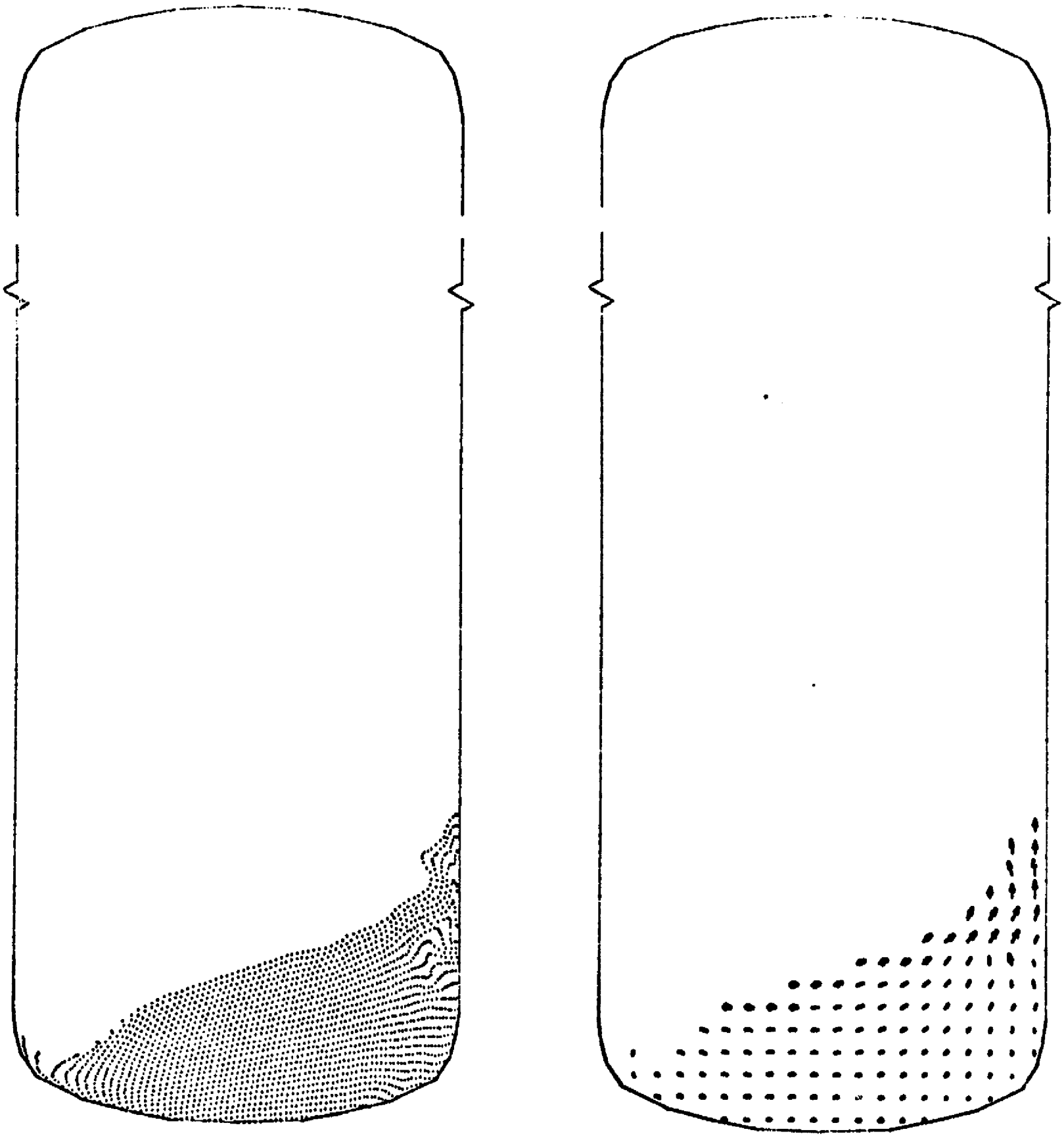

Example 1

Fig. 12 - Flow and Velocity Fields at t = 0.8 sec.

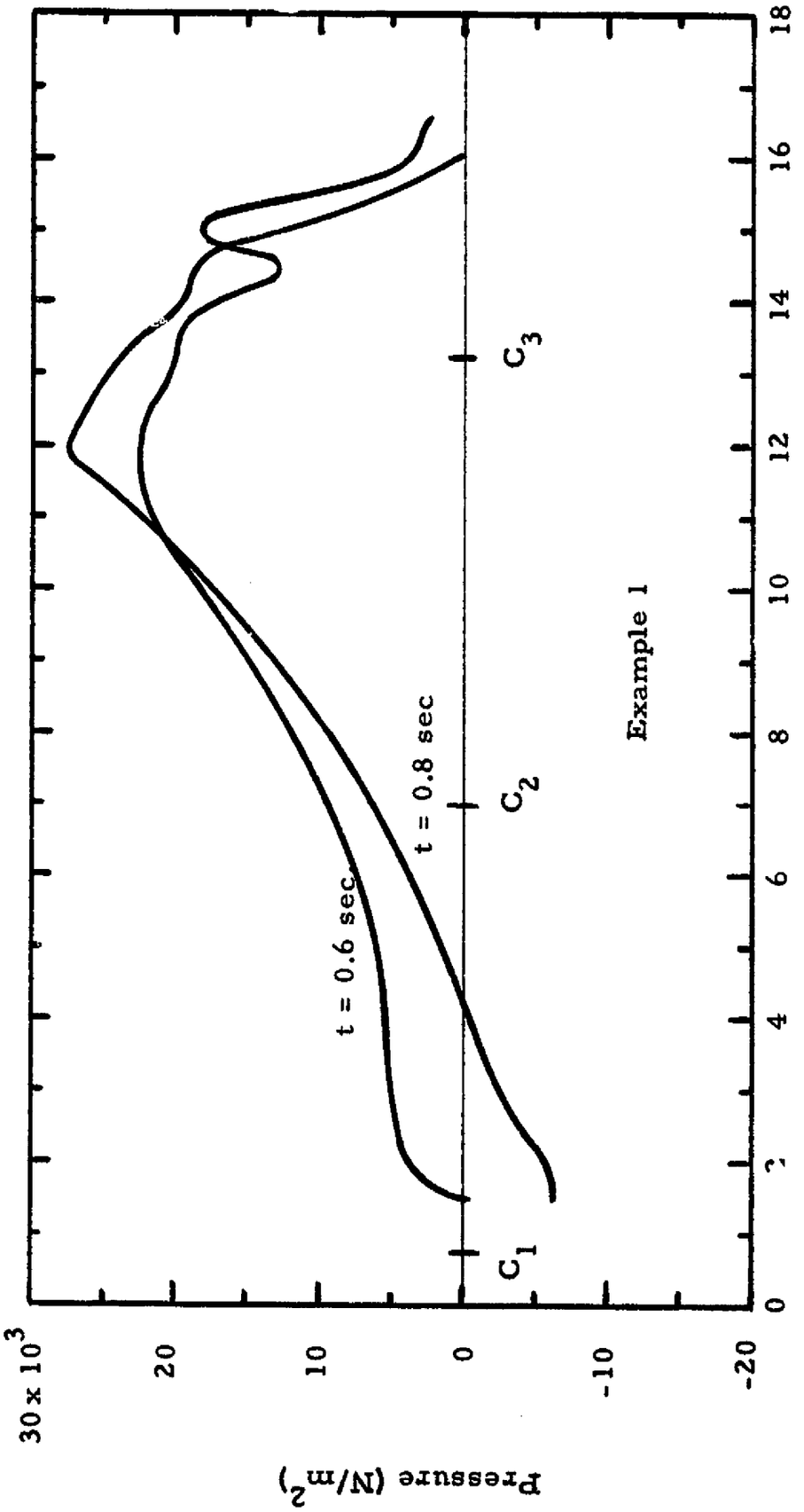

Fig. 13 - Pressure Distributions Along the Tank Wall at t = 0.6 and 0.8 sec. (See Fig. 8 for C_1, C_2 and C_3)

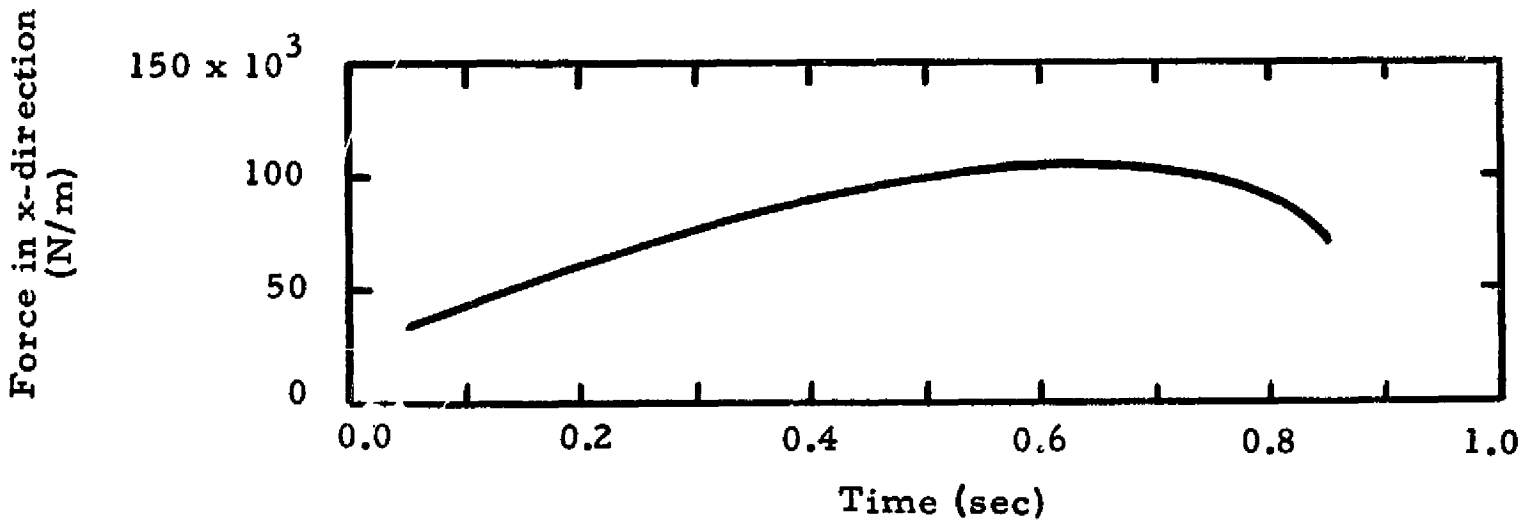

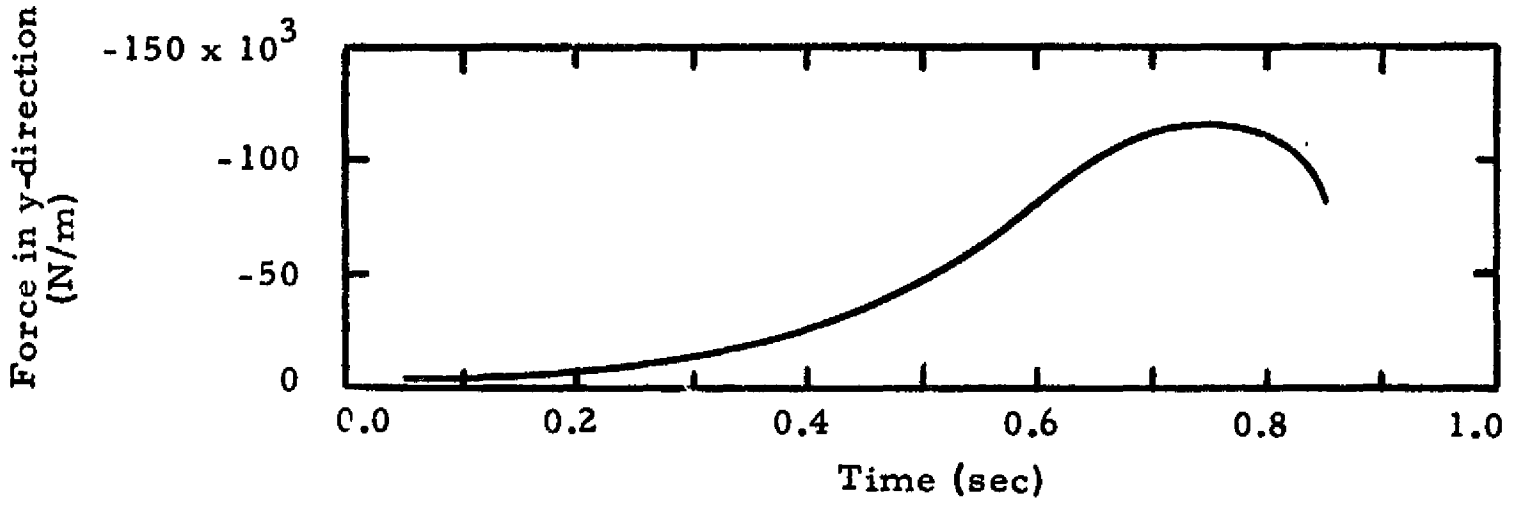

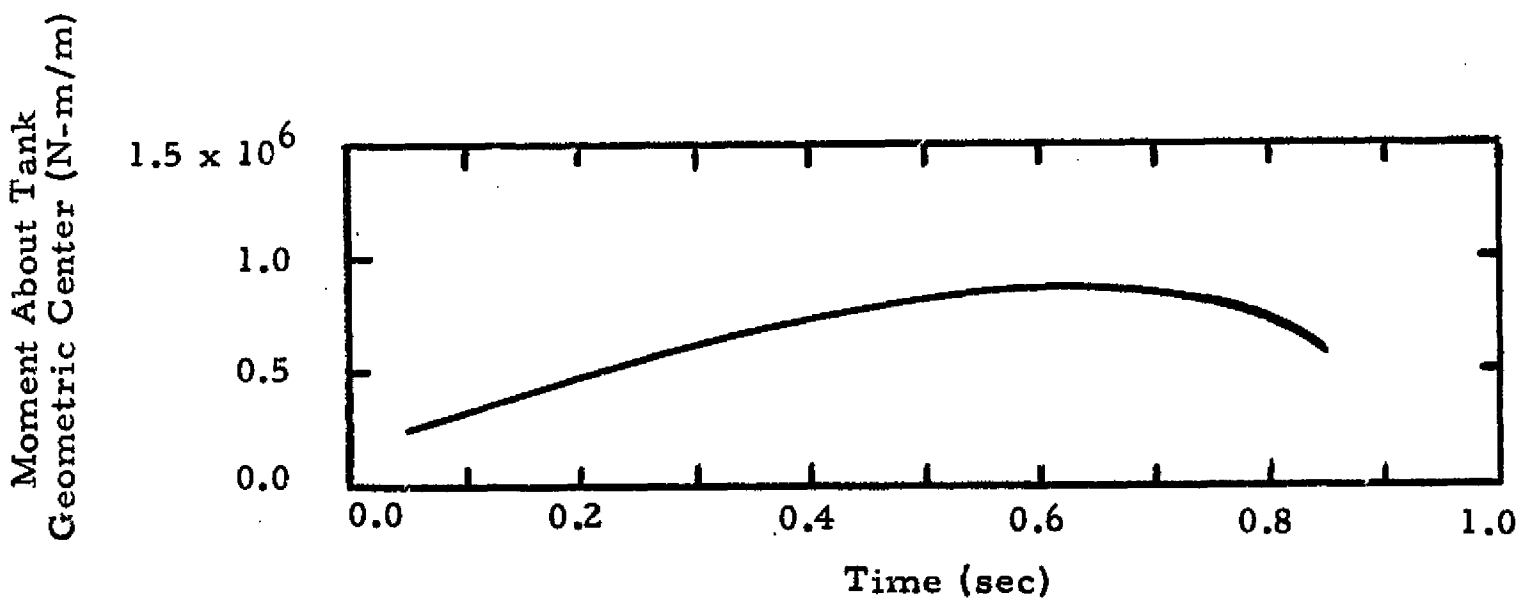

Example 1

Fig. 14 - Forces and Moment Exerted by the Propellant on the Container

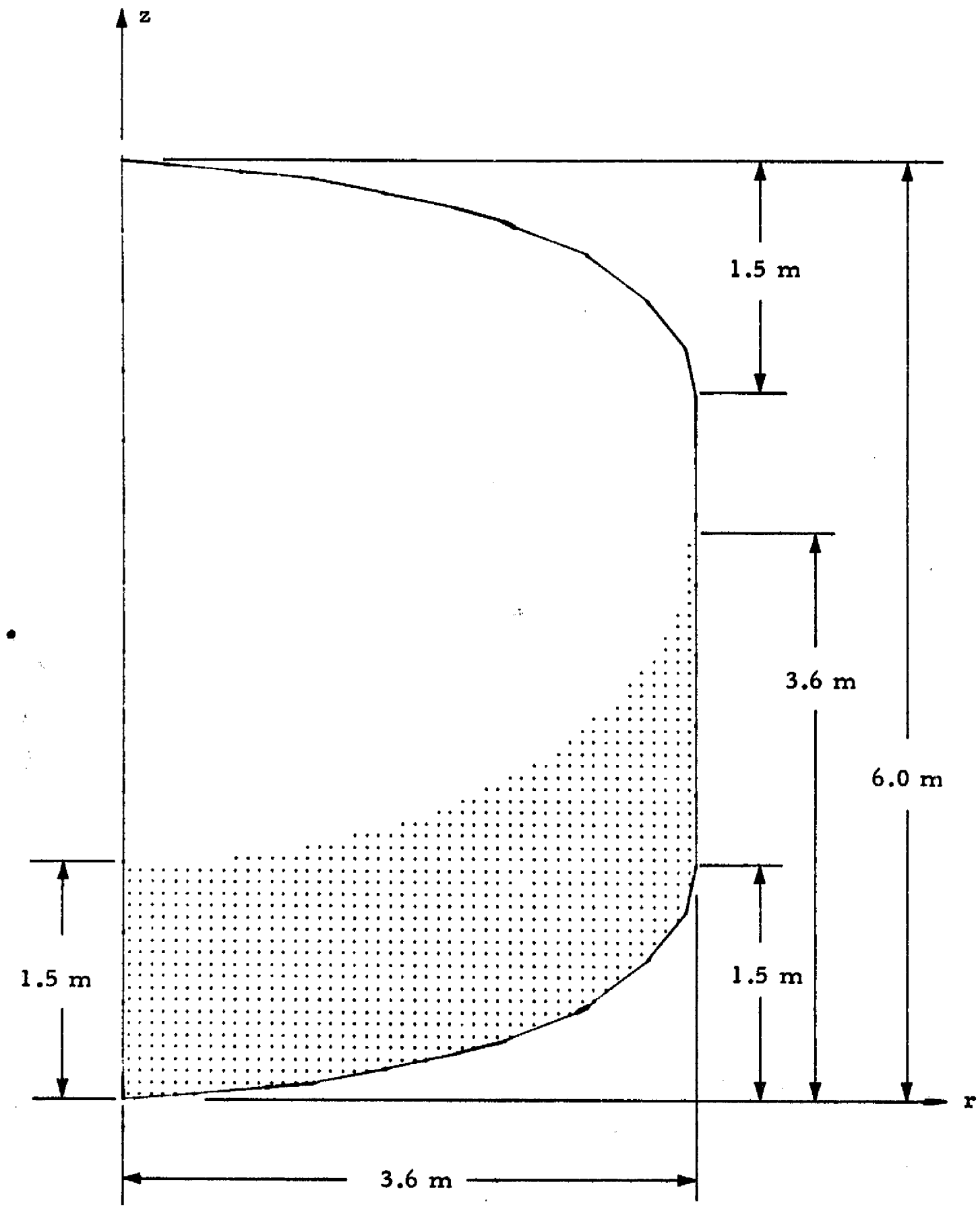

Example 2

Fig. 15 - Tank Geometry and Propellant Level

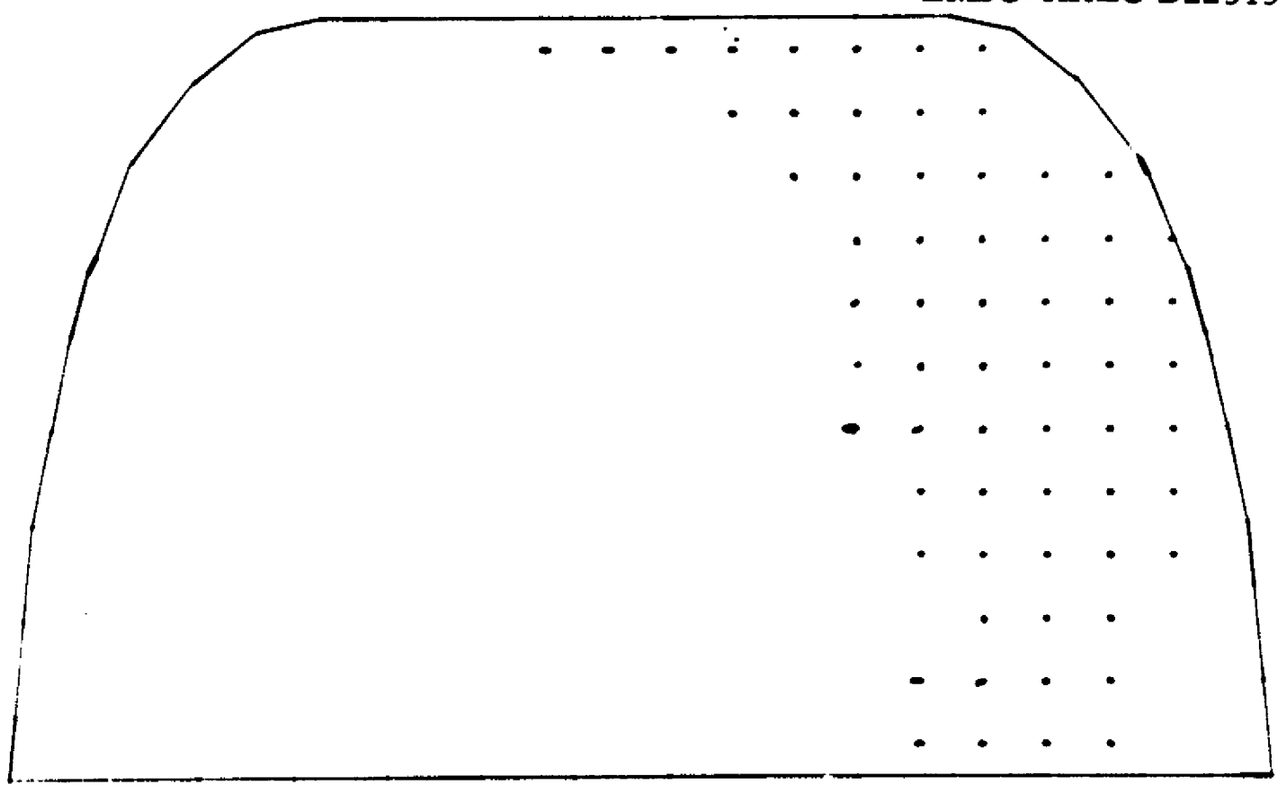

Example 2

Fig. 16 - Flow and Velocity Fields at t = 0.4 sec (Case A)

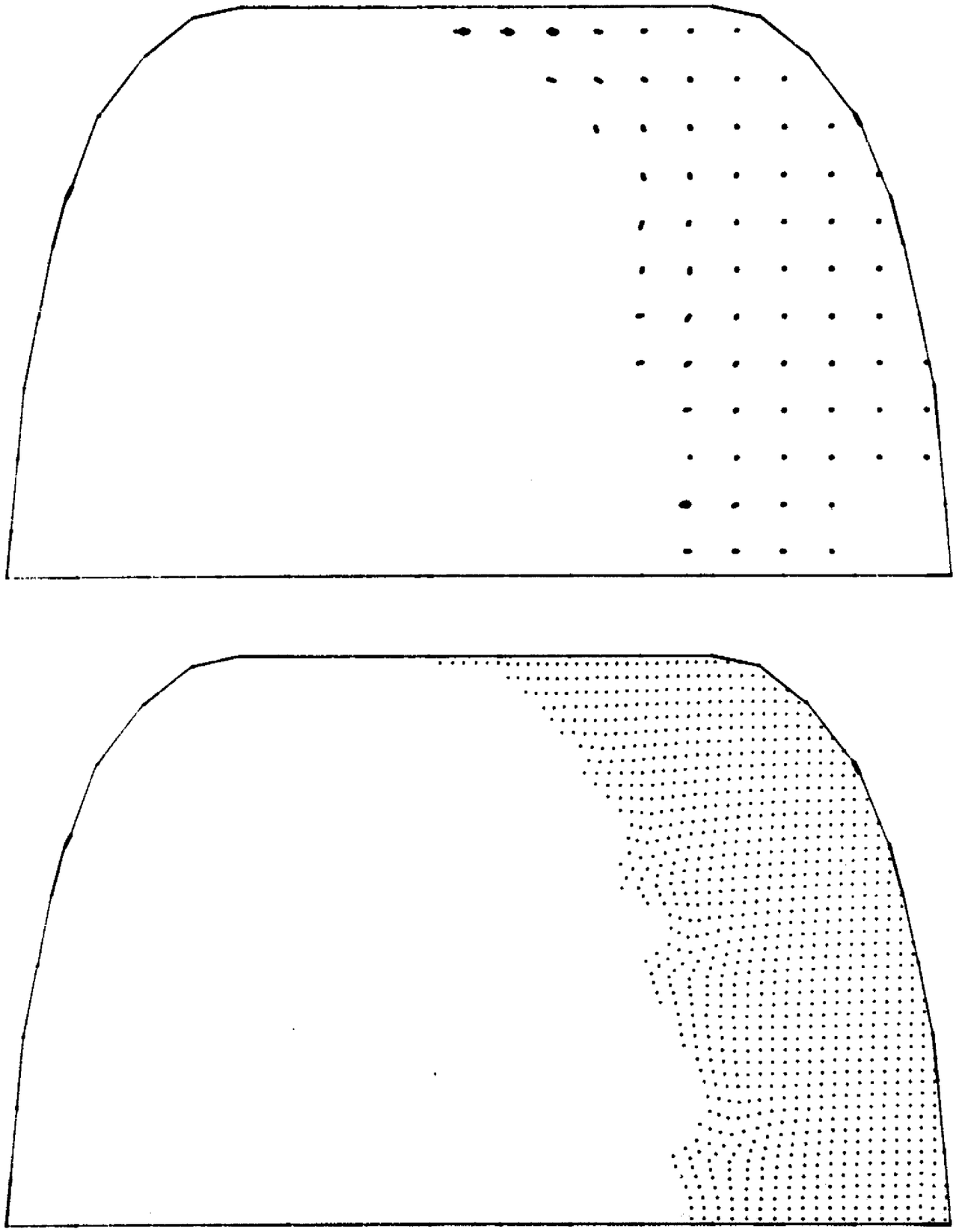

Example 2

Fig. 17 - Flow and Velocity Fields at t = 0.8 sec (Case A)

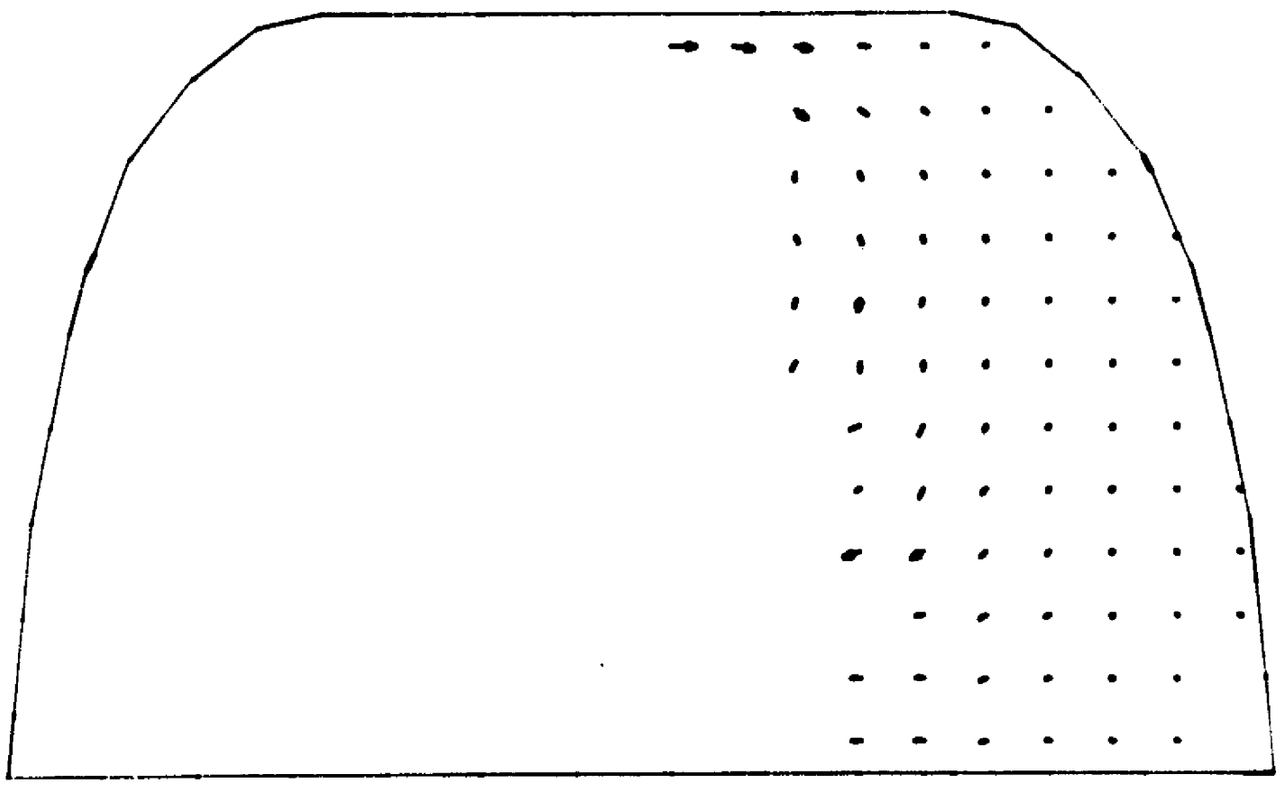

Example 2

Fig. 18 - Flow and Velocity Fields at t = 1.2 sec (Case A)

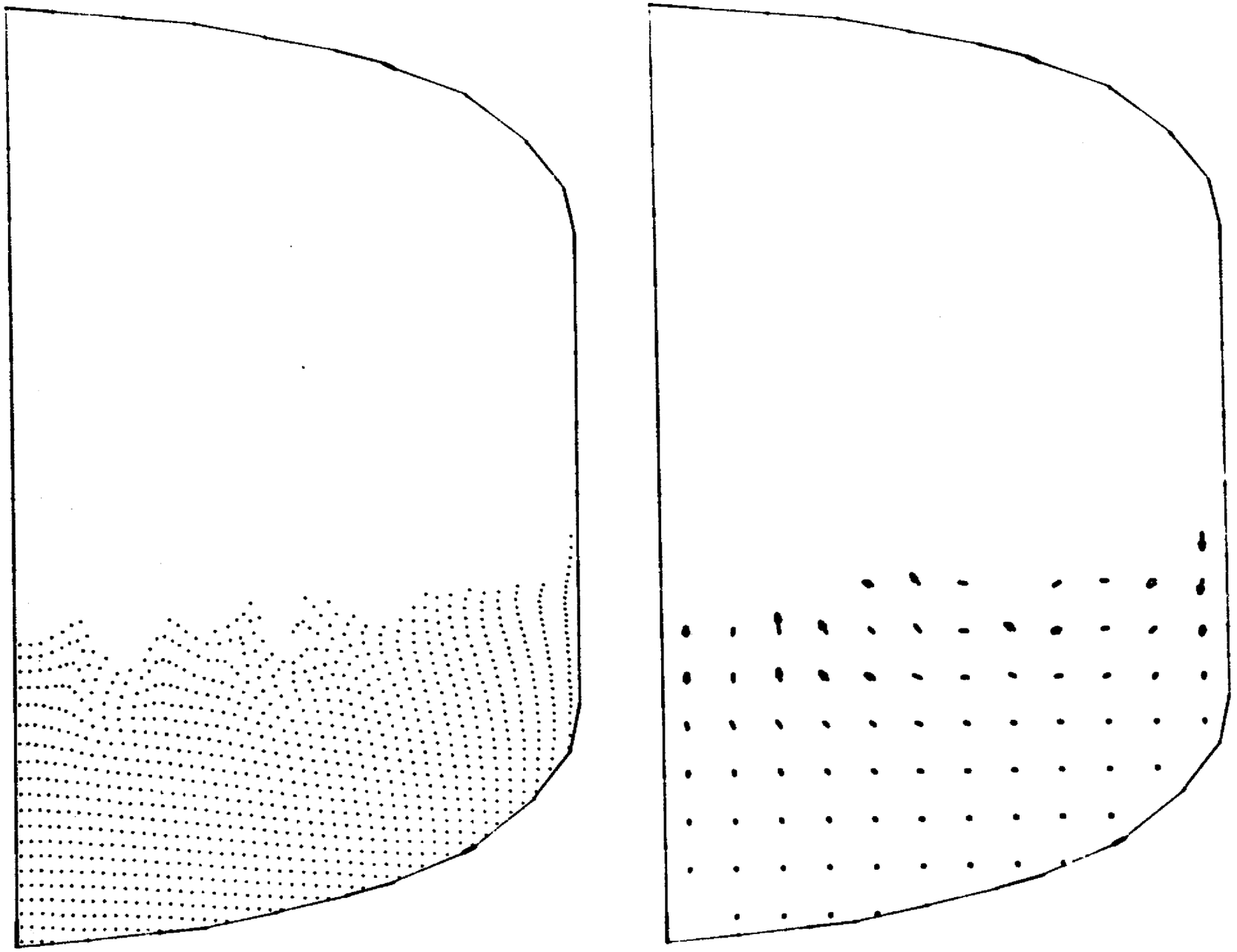

Example 2

Fig. 19 - Flow and Velocity Fields at t = 1.4 sec (Case A)

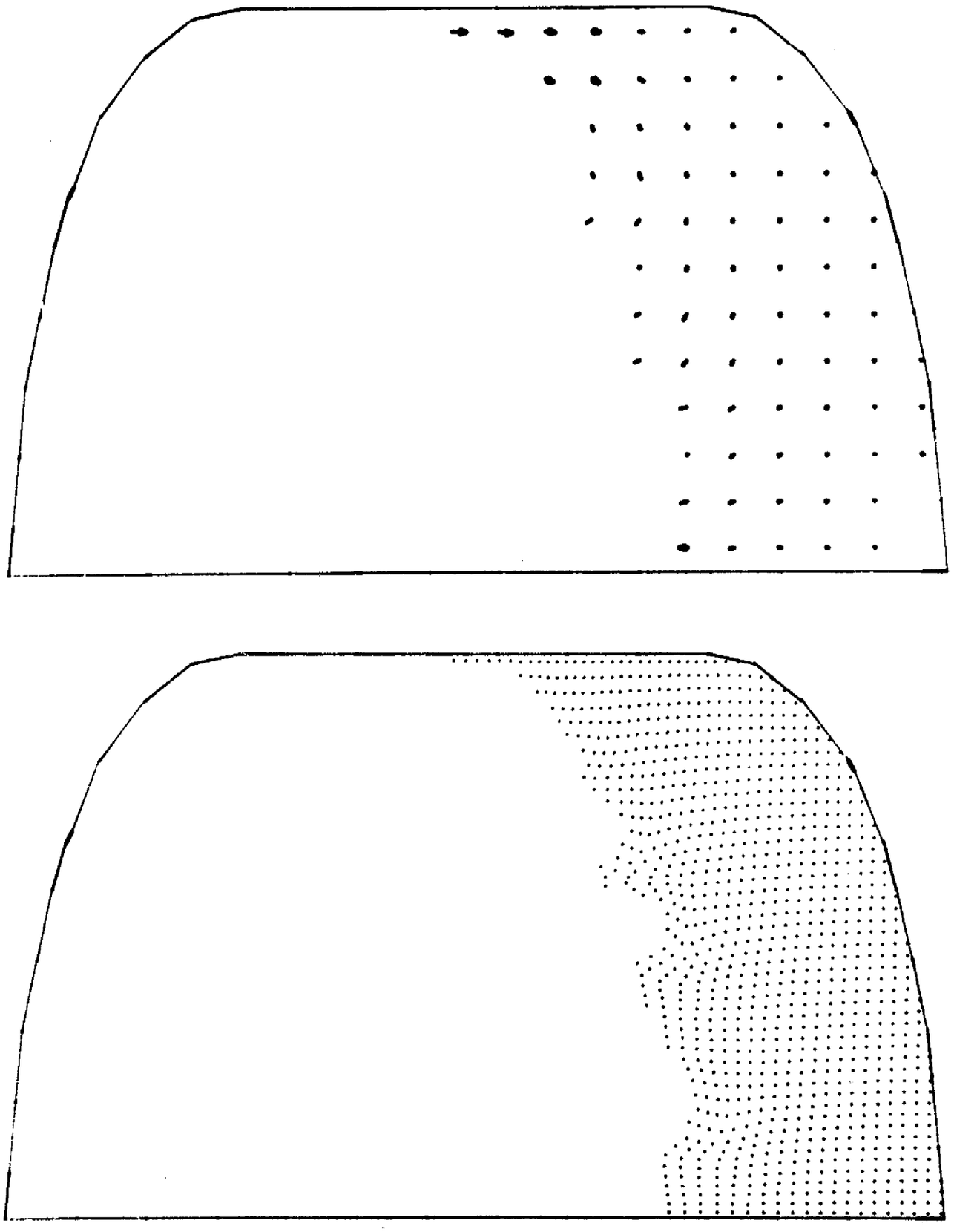

Example 2

Fig. 20 - Flow and Veloctiy Fields at t = 0.4 sec (Case B)

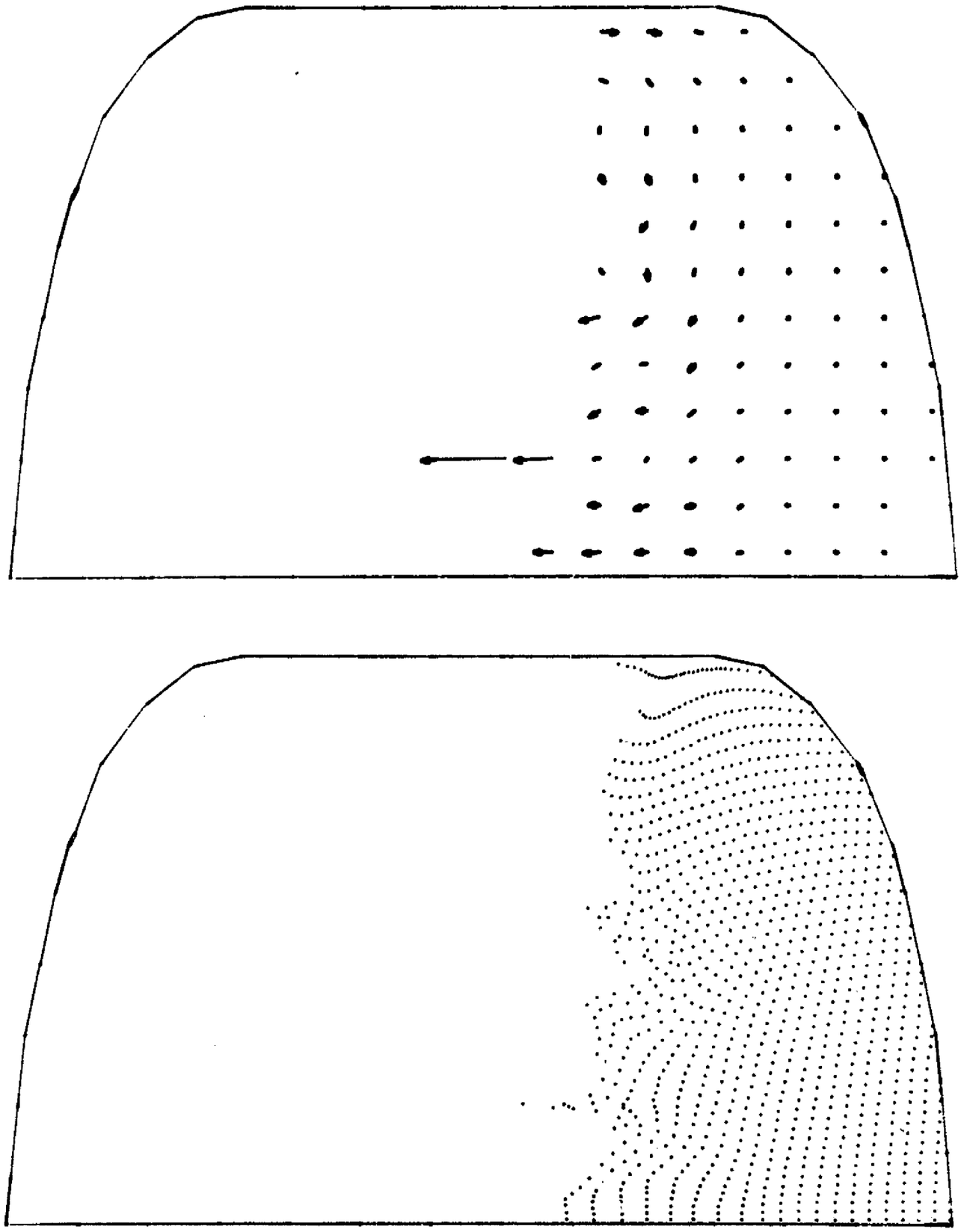

Example 2

Fig. 21 - Flow and Velocity Fields at t = 0.8 sec (Case B)

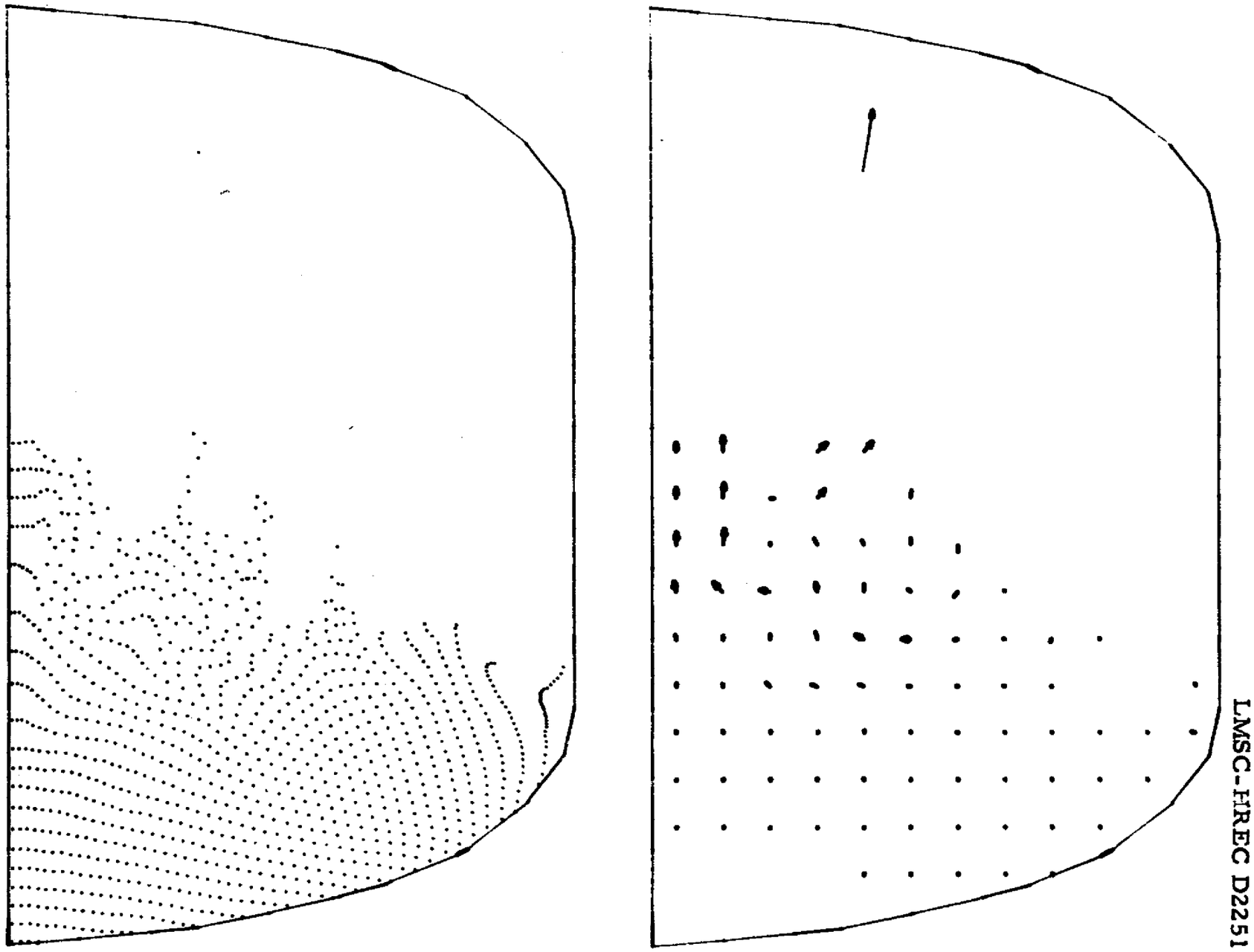

Example 2

Fig. 22 - Flow and Velocity Fields at t = 1.2 sec (Case B)

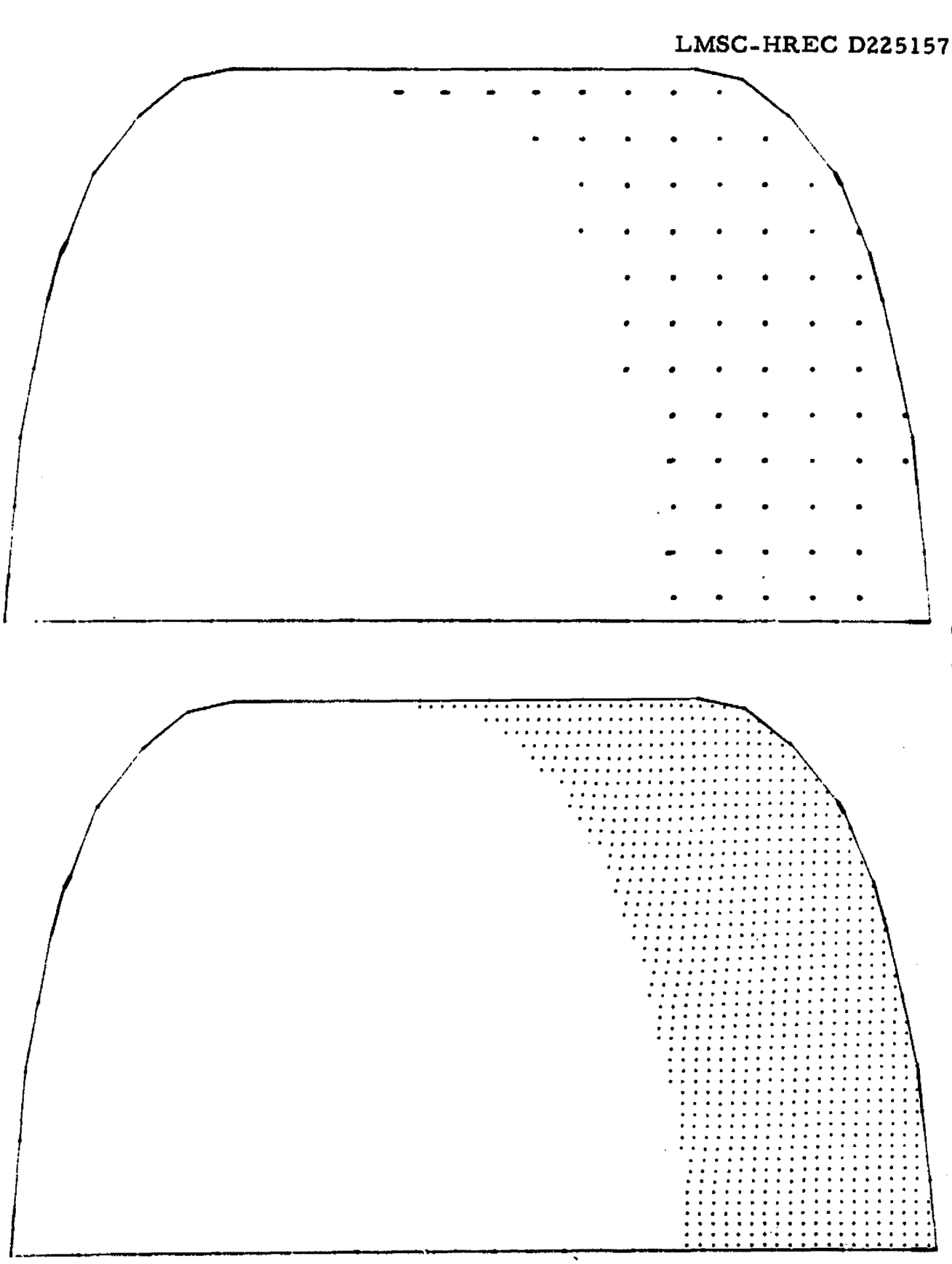

Example 2

Fig. 23 - Flow and Velocity Fields at t = 0.8 sec (Case C)

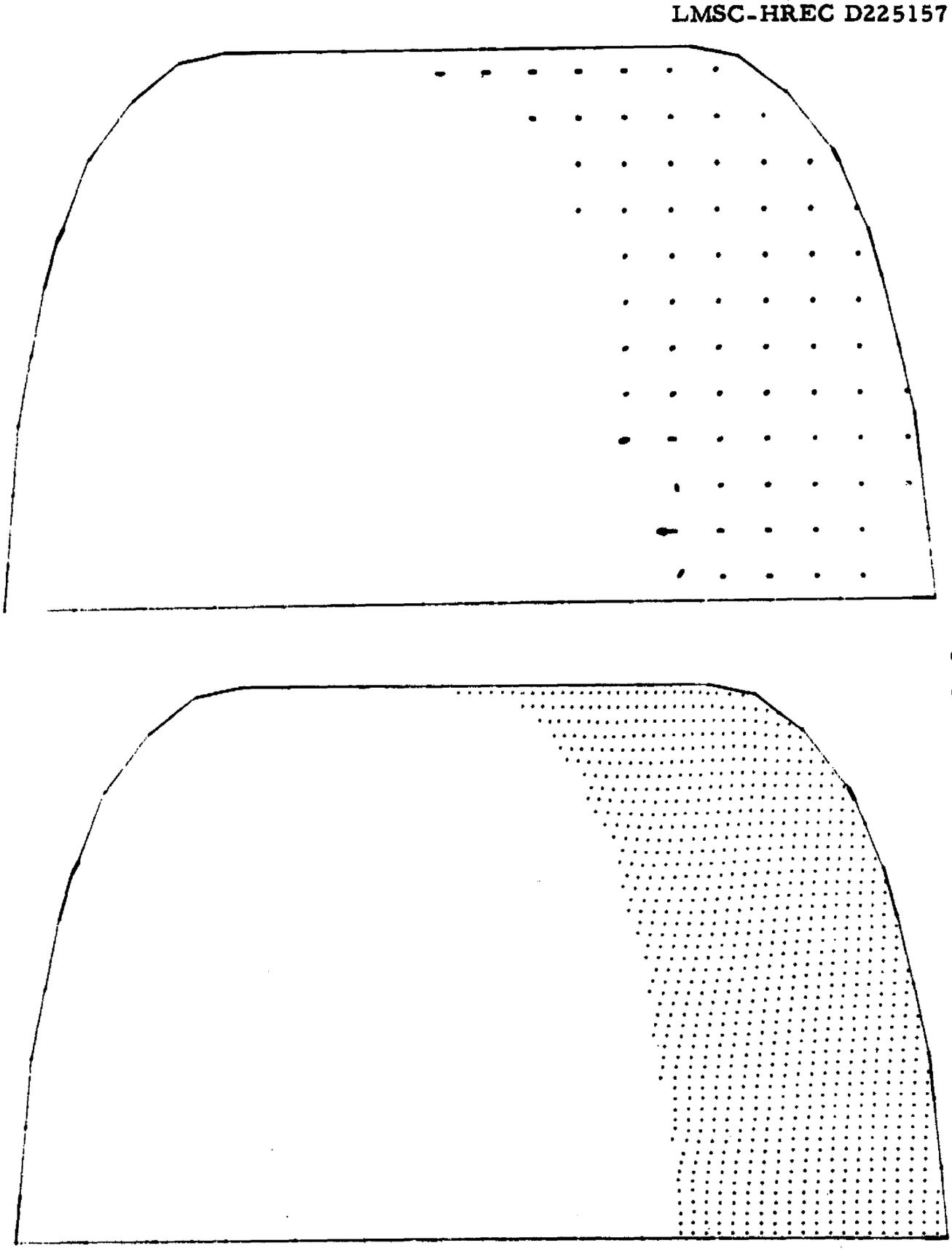

Example 2

Fig. 24 - Flow and Velocity Fields at t = 1.2 sec (Case C)

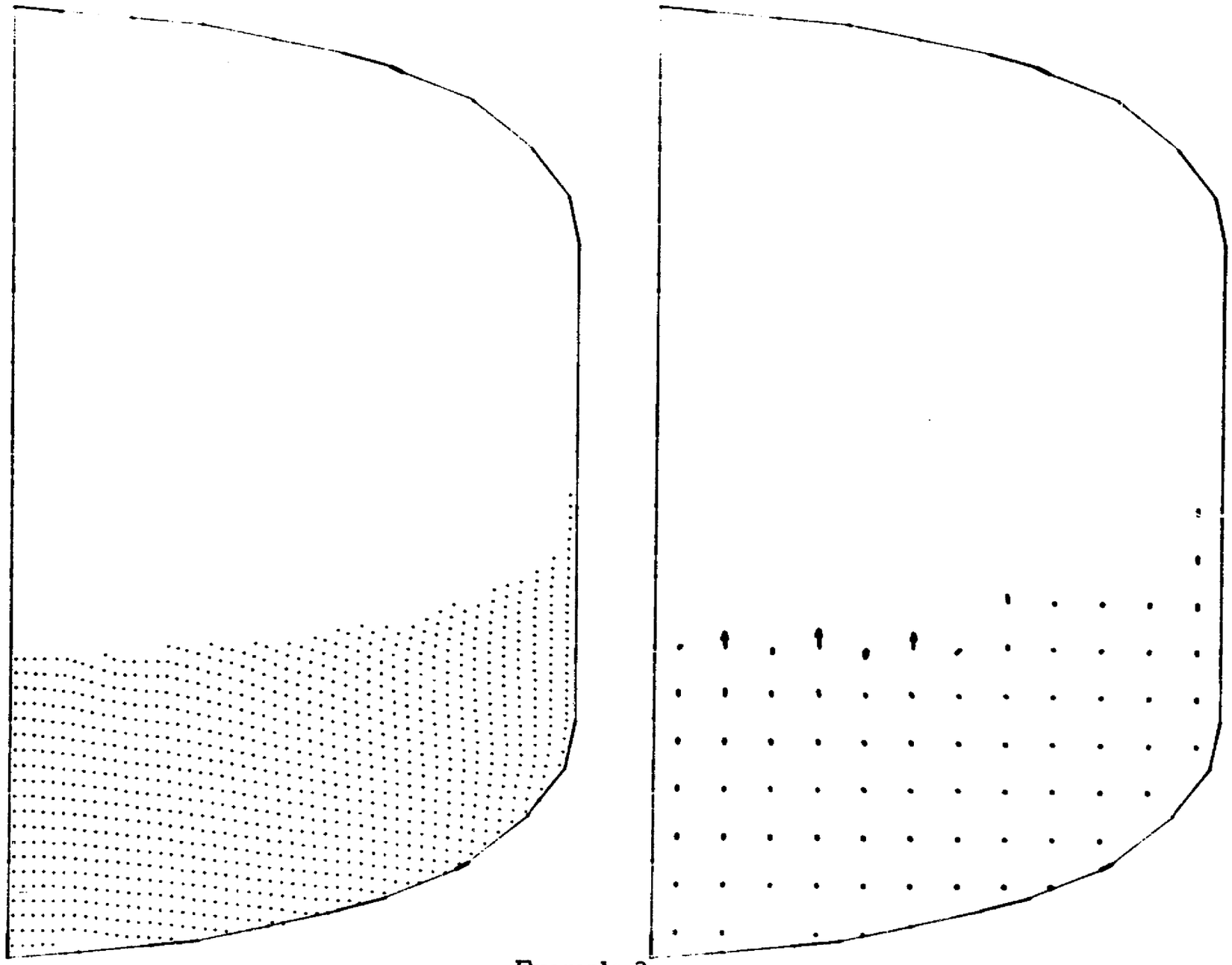

Example 2

Fig. 25 - Flow and Velocity Fields at t = 1.6 sec (Case C)

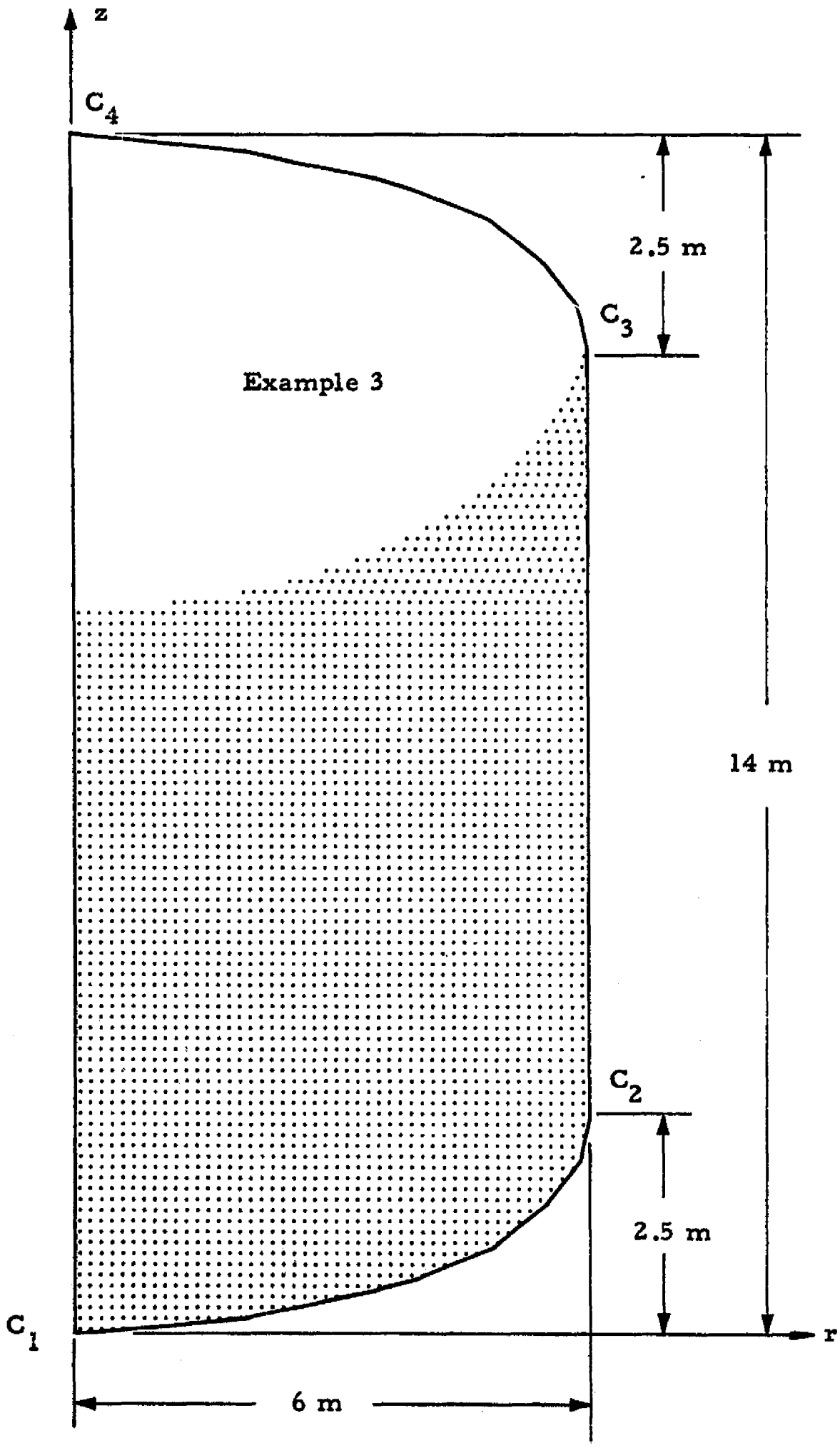

Fig. 26 - Tank Geometry and Propellant Level (Sample Problem I)

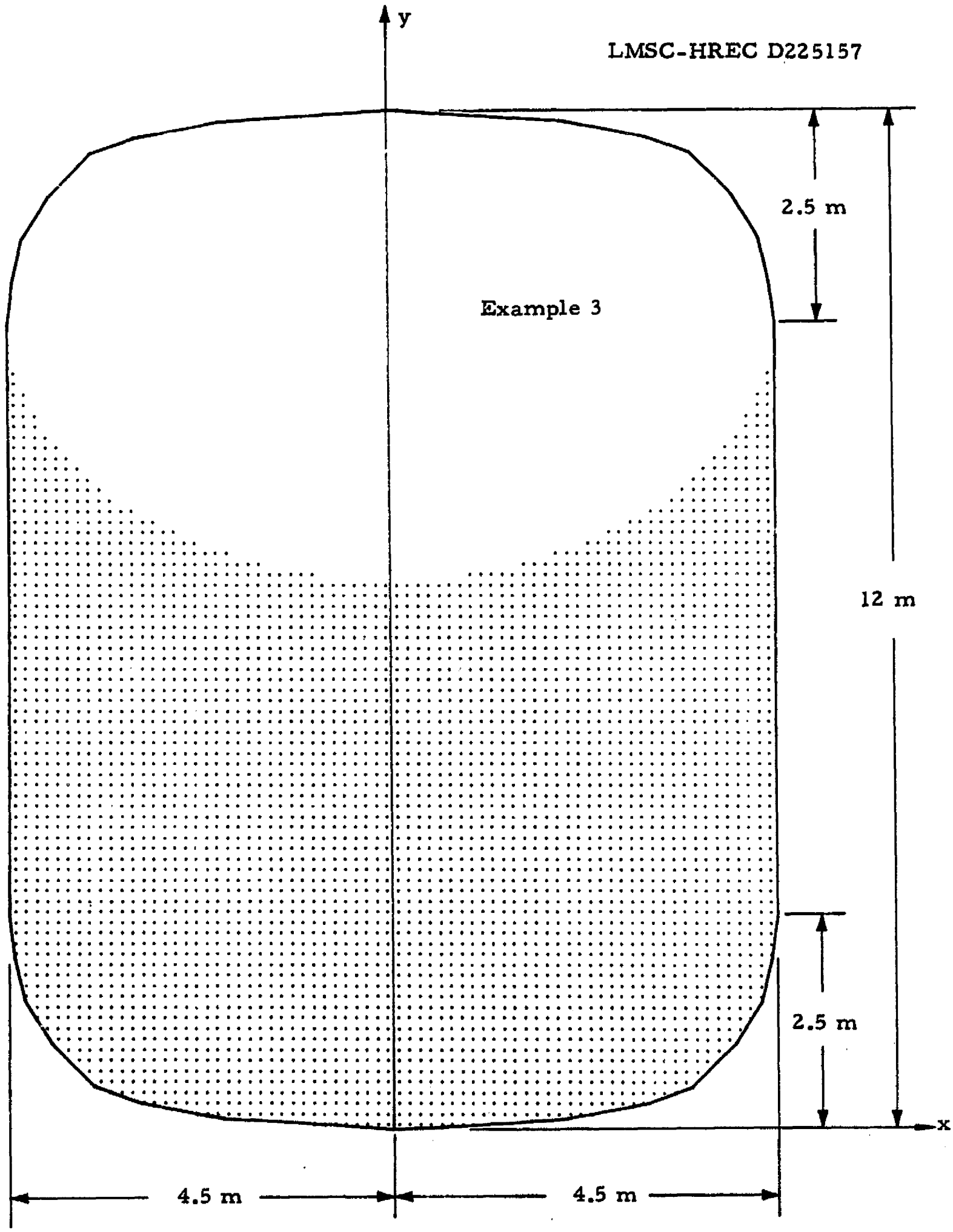

Fig. 27 - Tank Geometry and Propellant Level (Sample Problem II)

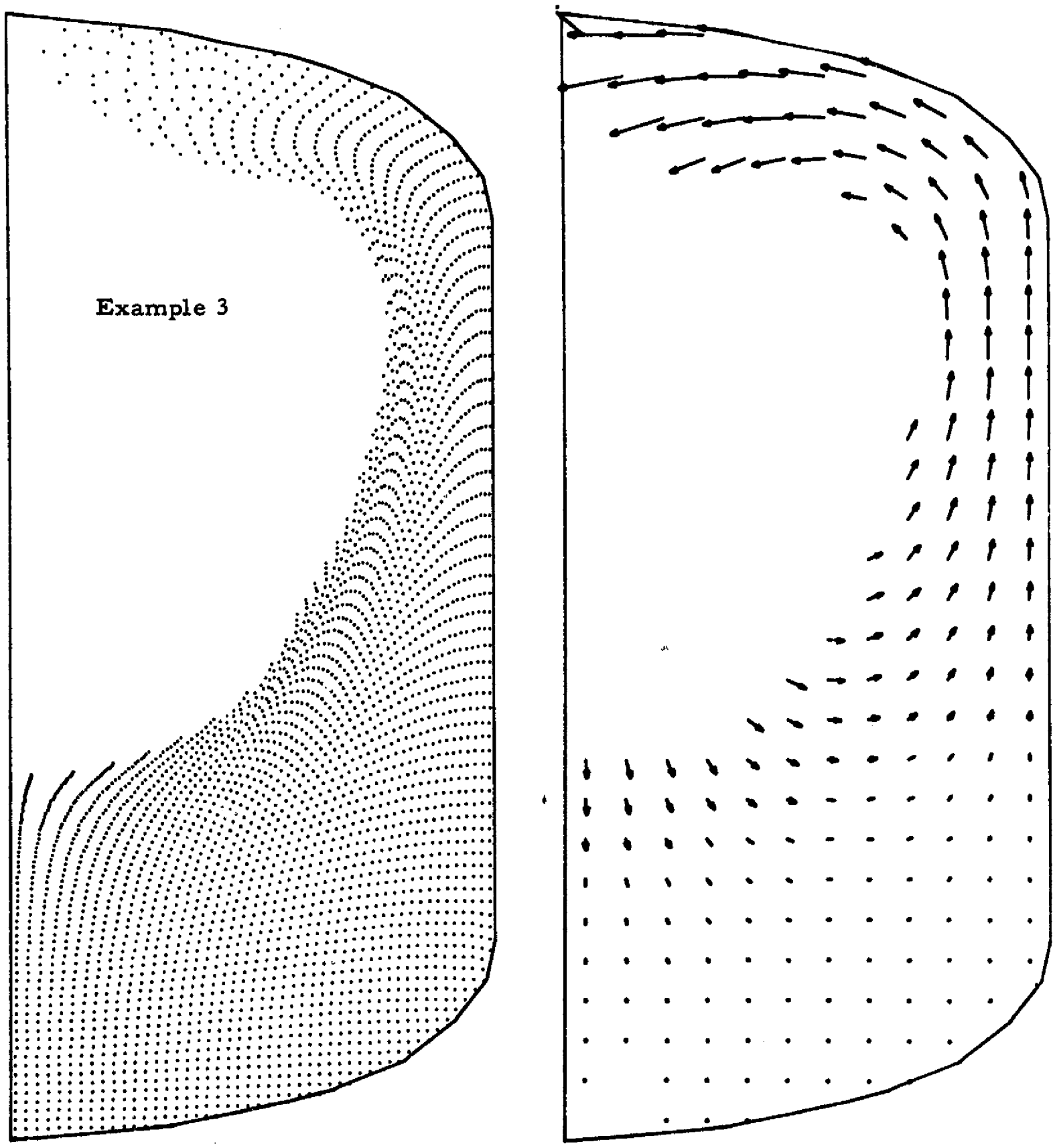

Fig. 28 - Flow and Velocity Fields at t = 5.0 sec (Sample Problem I)

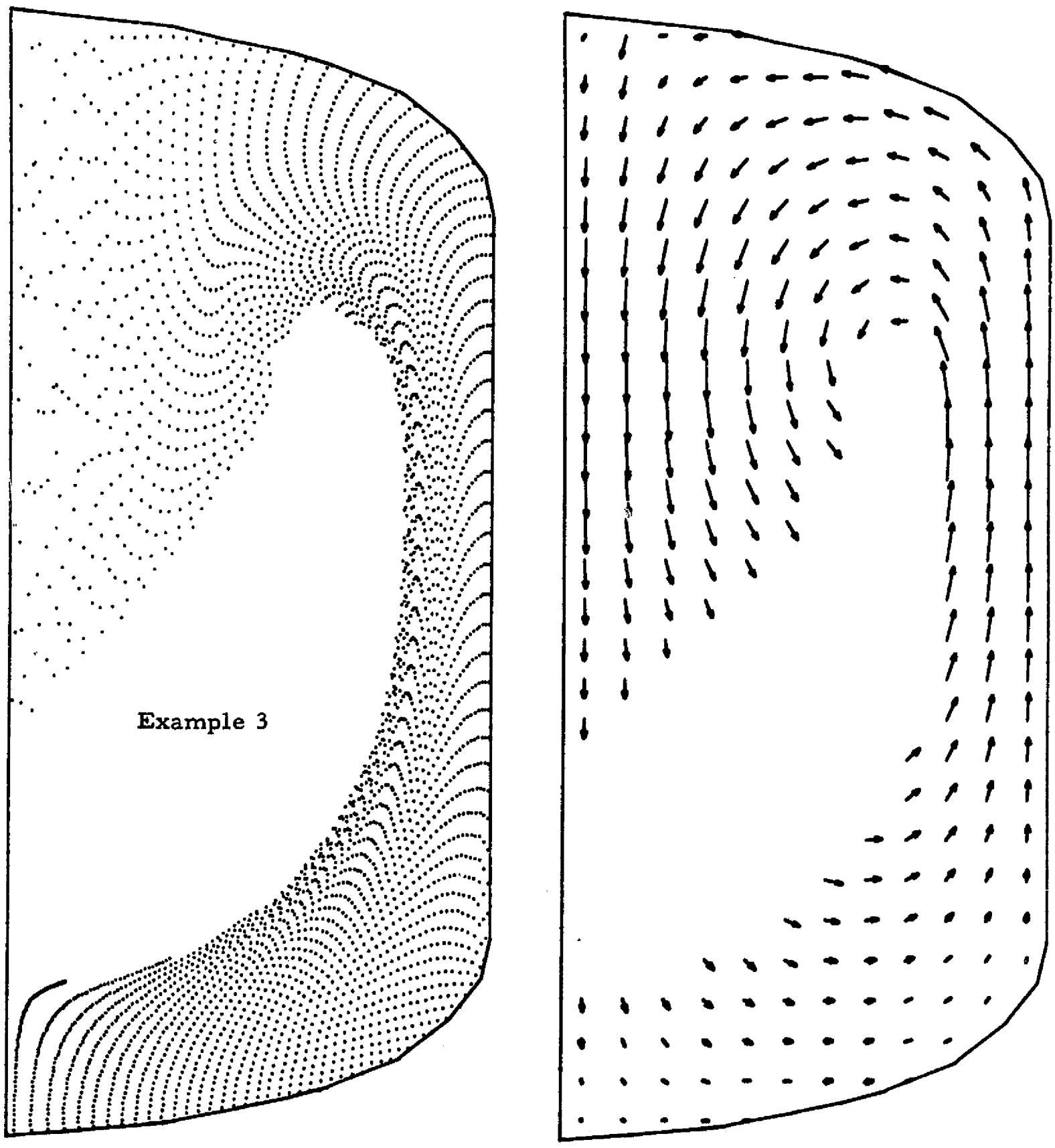

Fig. 29 - Flow and Velocity Fields at t = 8.0 sec (Sample Problem I)

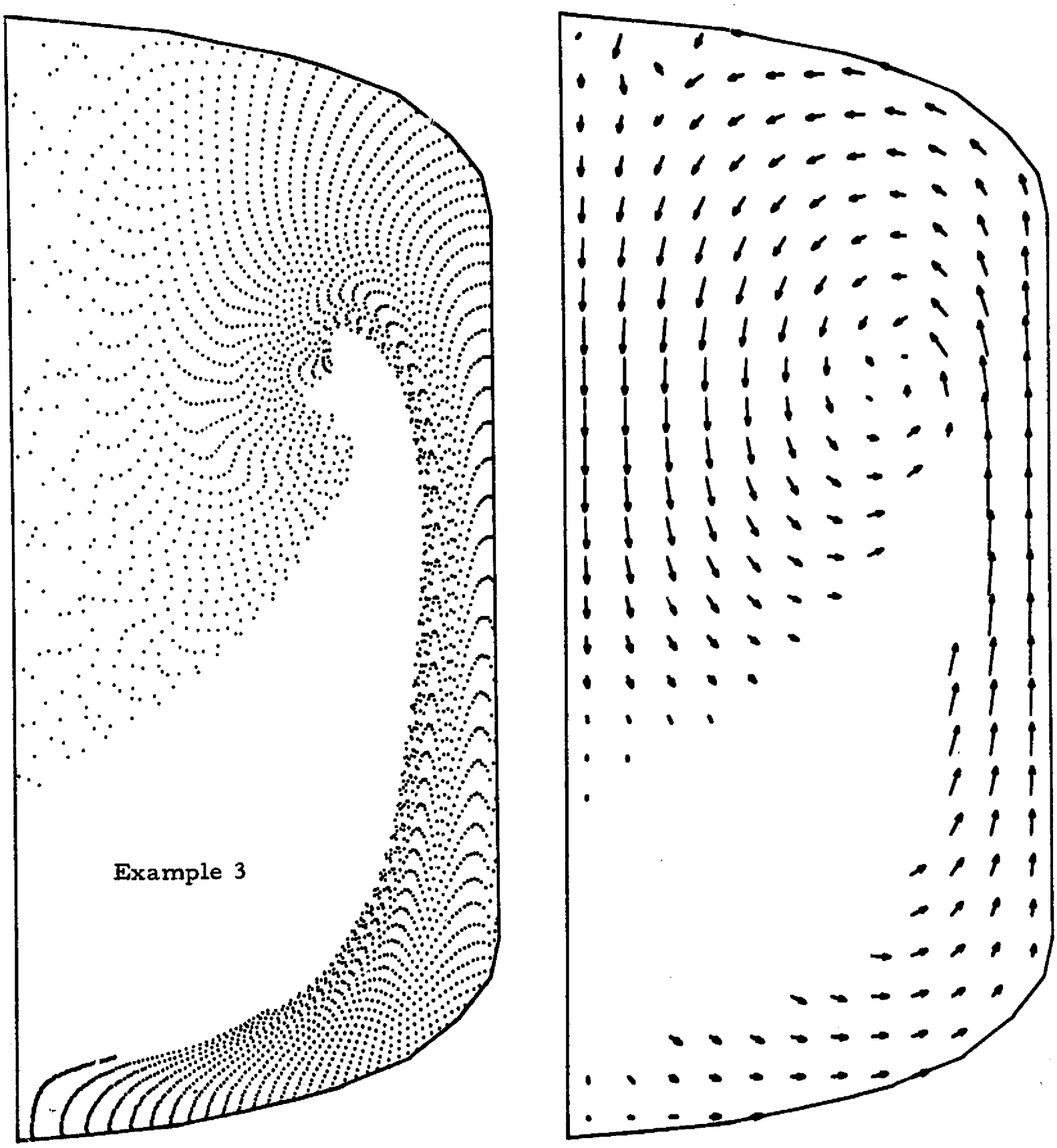

Fig. 30 - Flow and Velocity Fields at t = 9.5 sec (Sample Problem I)

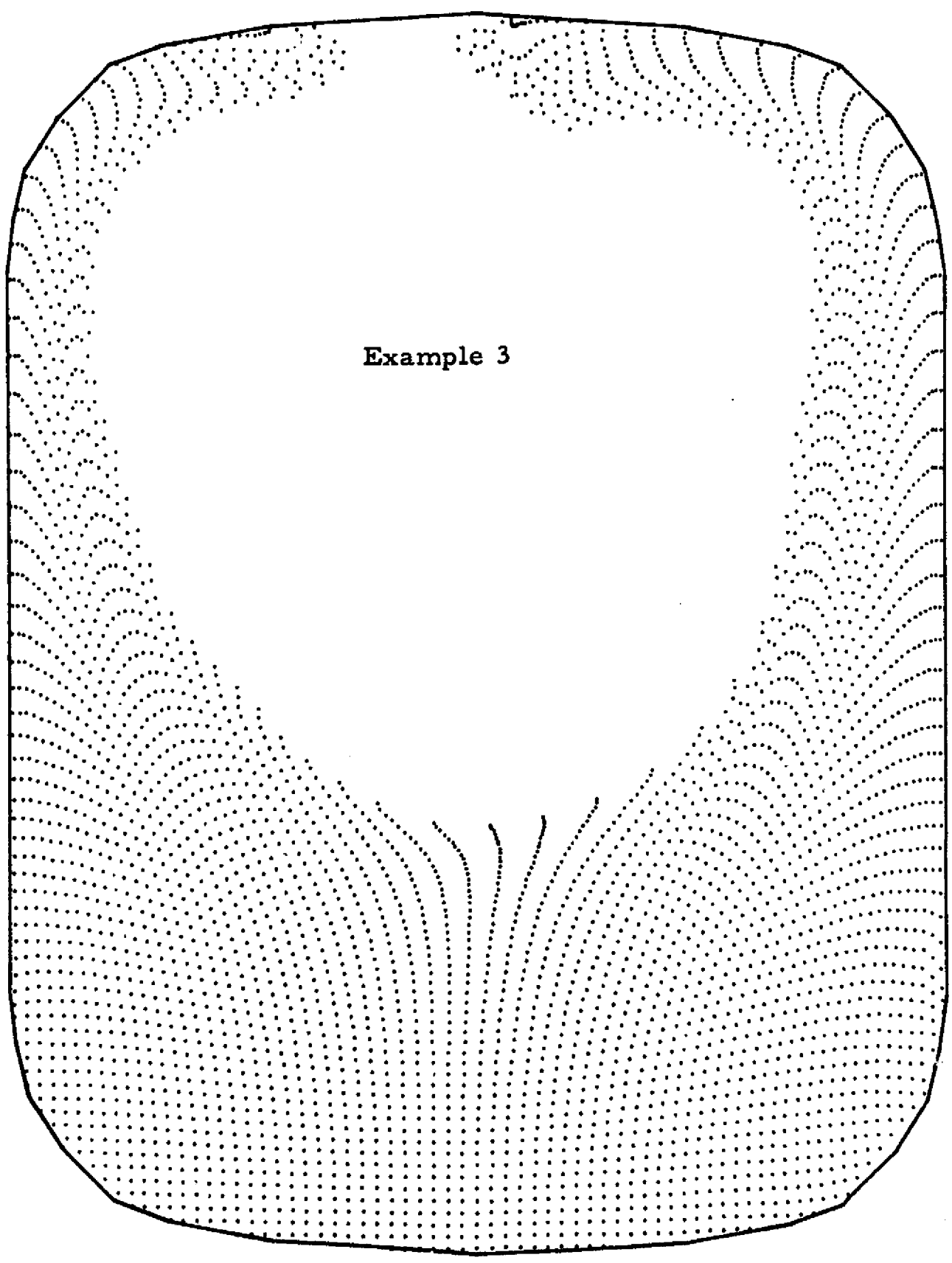

Fig. 31 - Flow Field of Sample Problem II (at t = 5.0 sec)

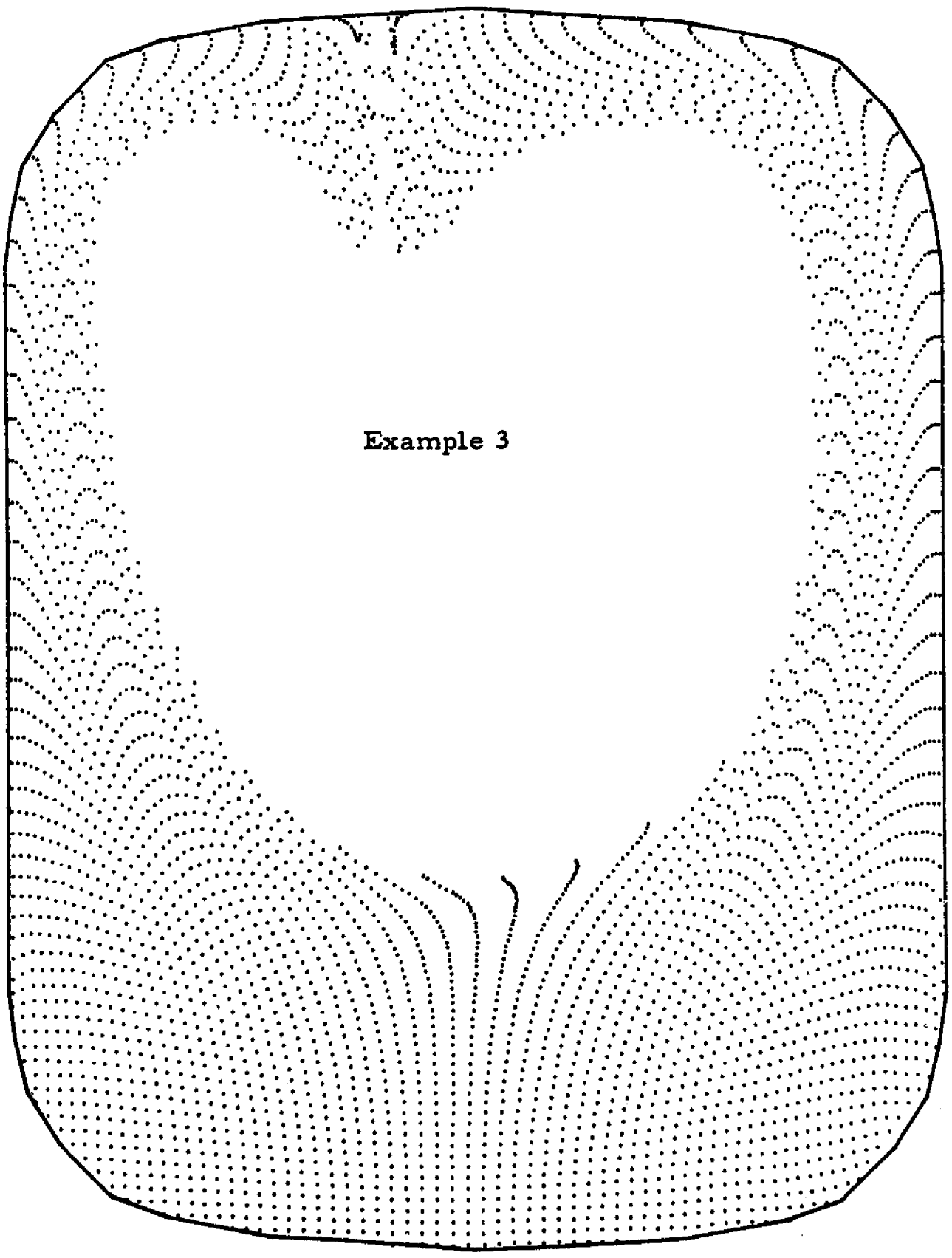

Example 3

Fig. 31 - Continued (at t = 6.0 sec)

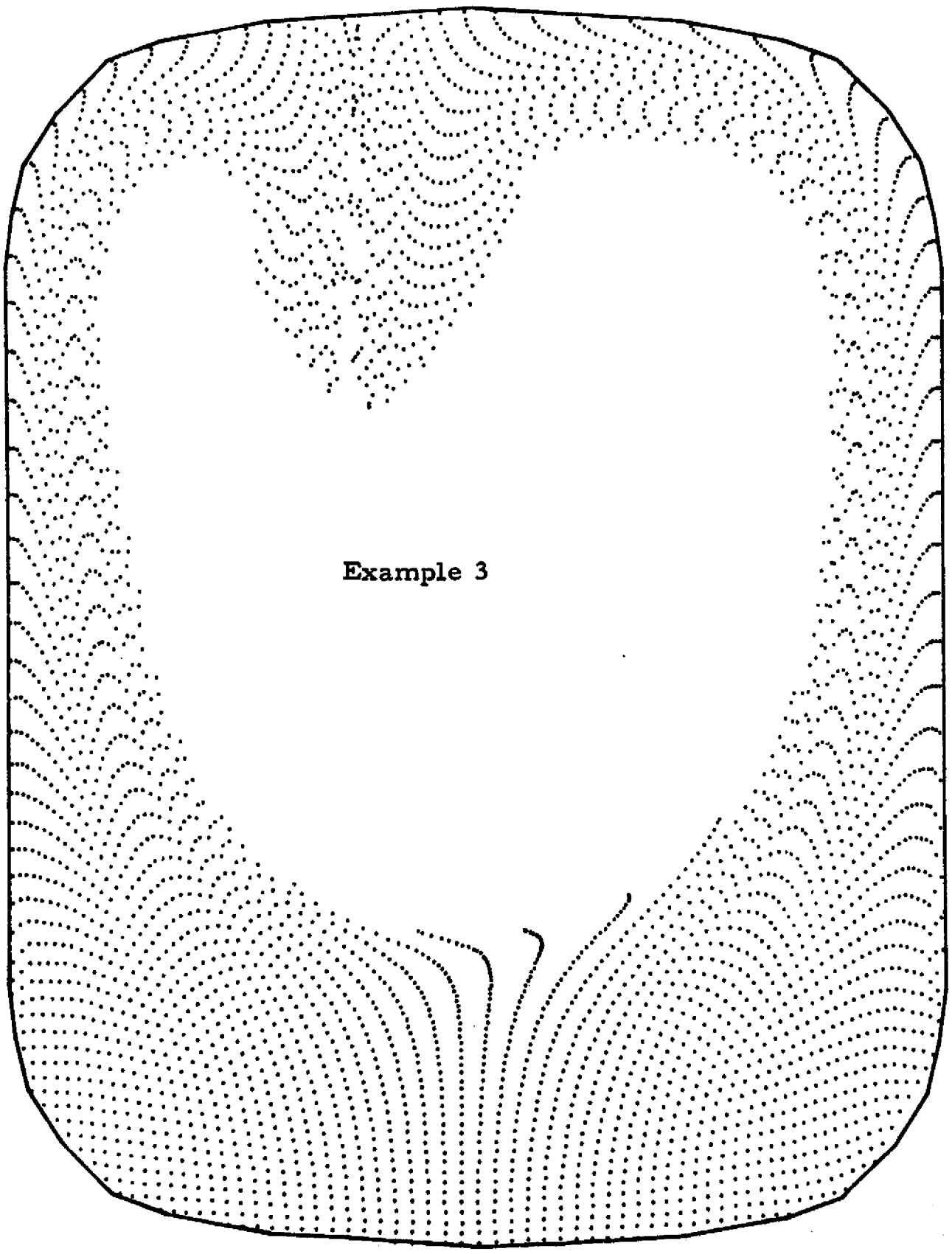

Example 3

Fig. 31 Continued (at t = 7.0 sec)

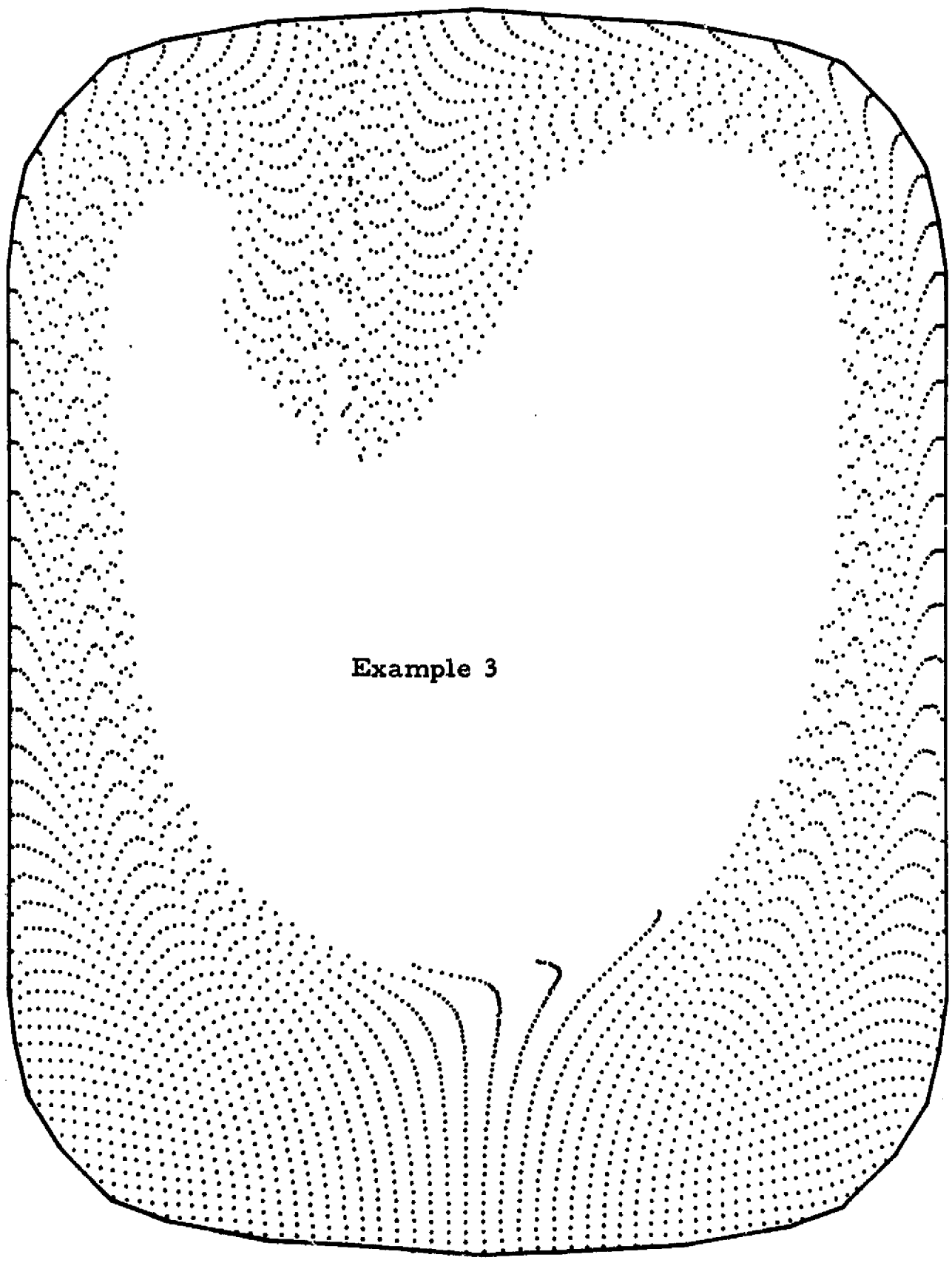

Fig. 31 Continued (at t = 7.5 sec)

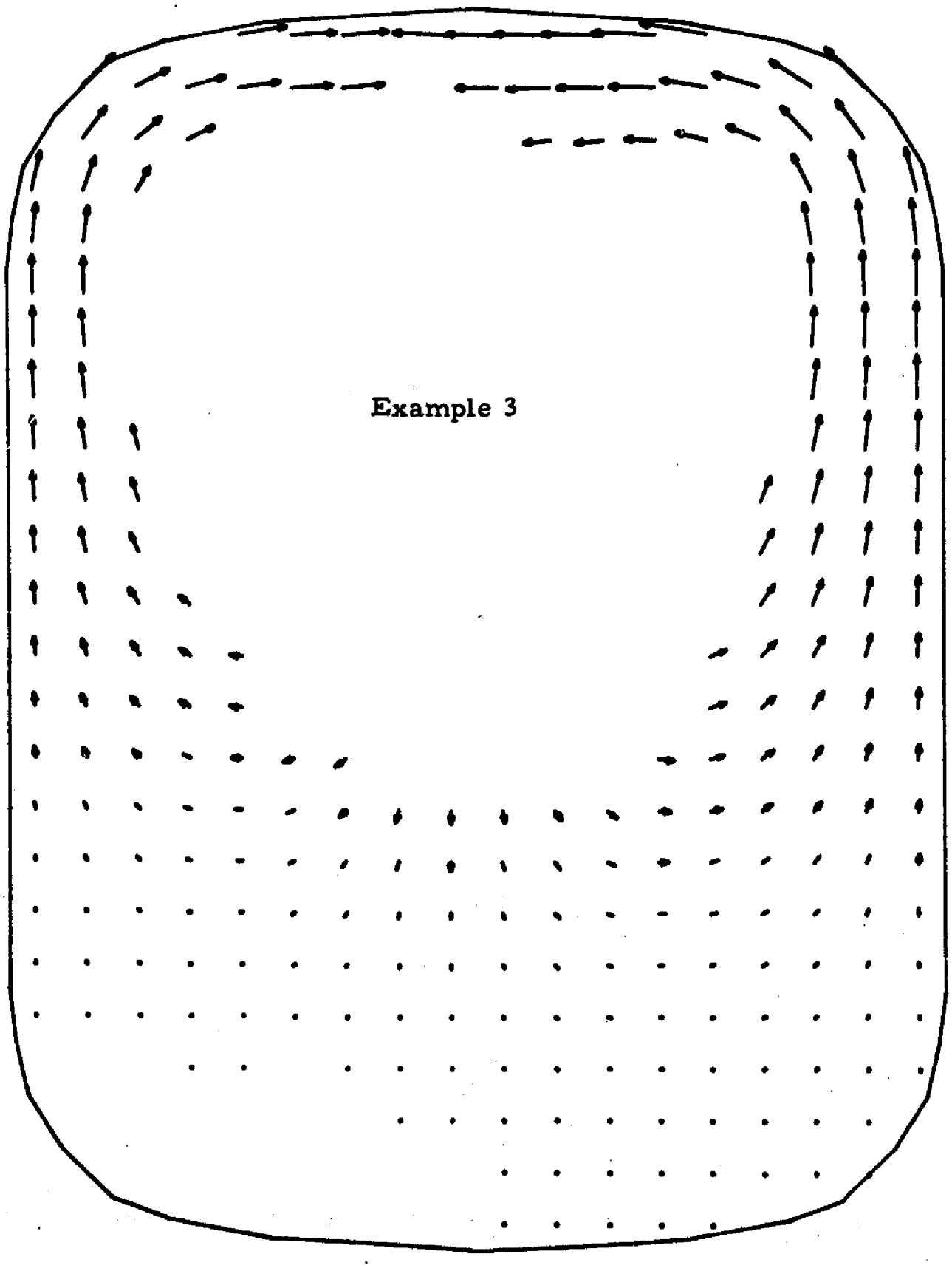

Example 3

Fig. 32 - Velocity Field of Sample Problem II (at t = 5.0 sec)

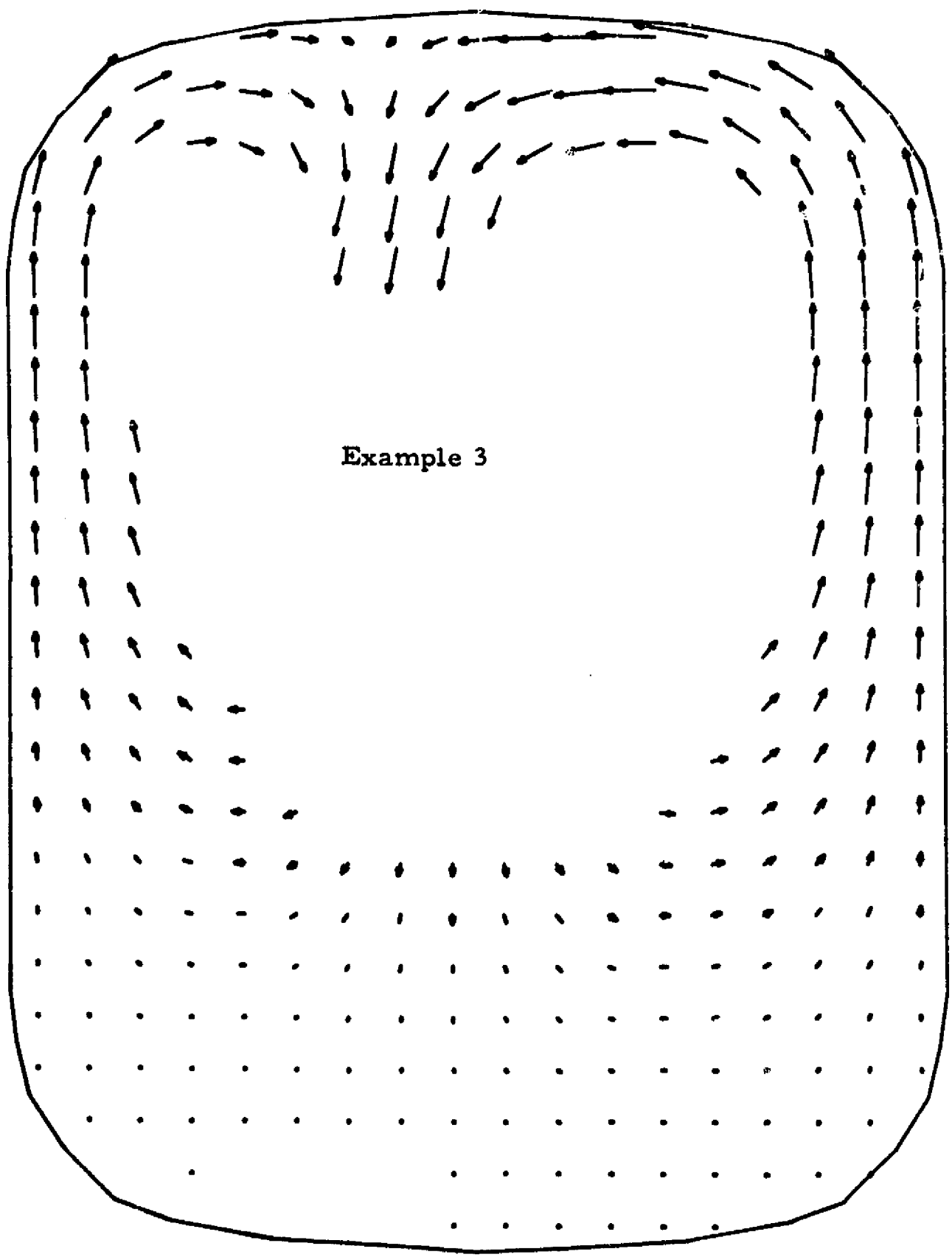

Fig. 32 Continued (at t = 6.0 sec)

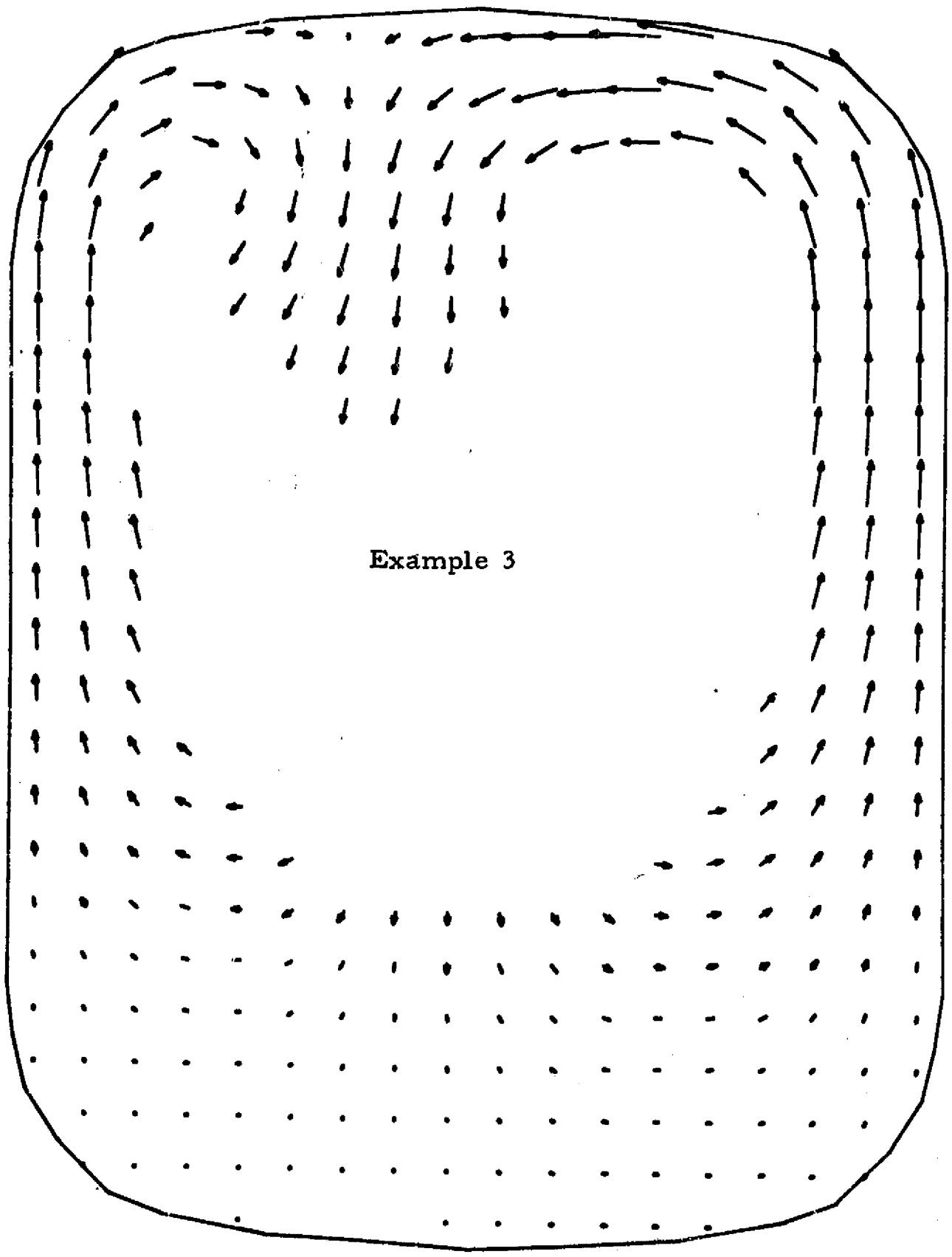

Example 3

Fig. 32 Continued (at t = 7.0 sec)

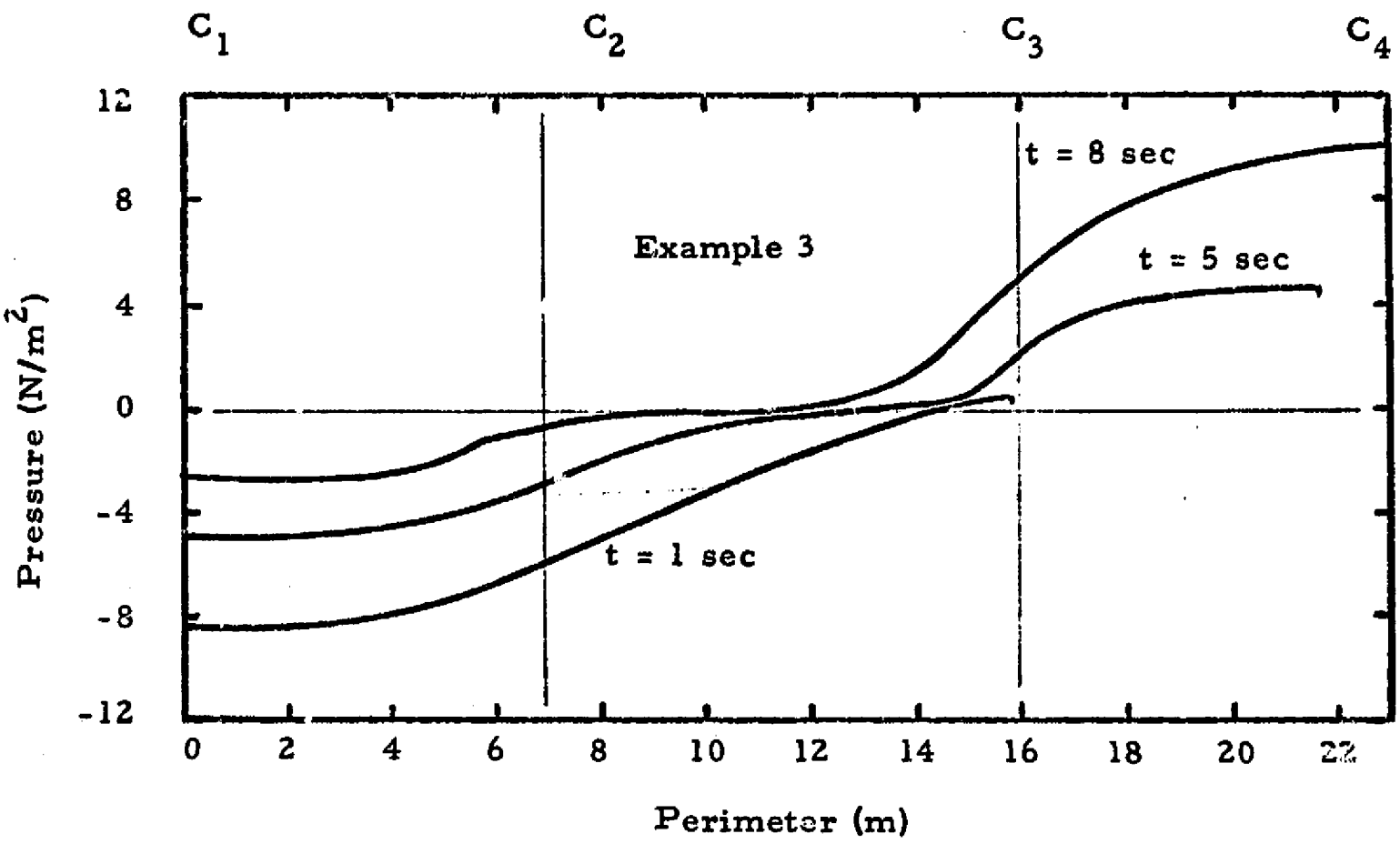

Fig. 33 - Pressure Distribution Along the Tank Wall (Sample Problem I)
(See Fig. 26 for C_1, C_2, C_3 and C_4)

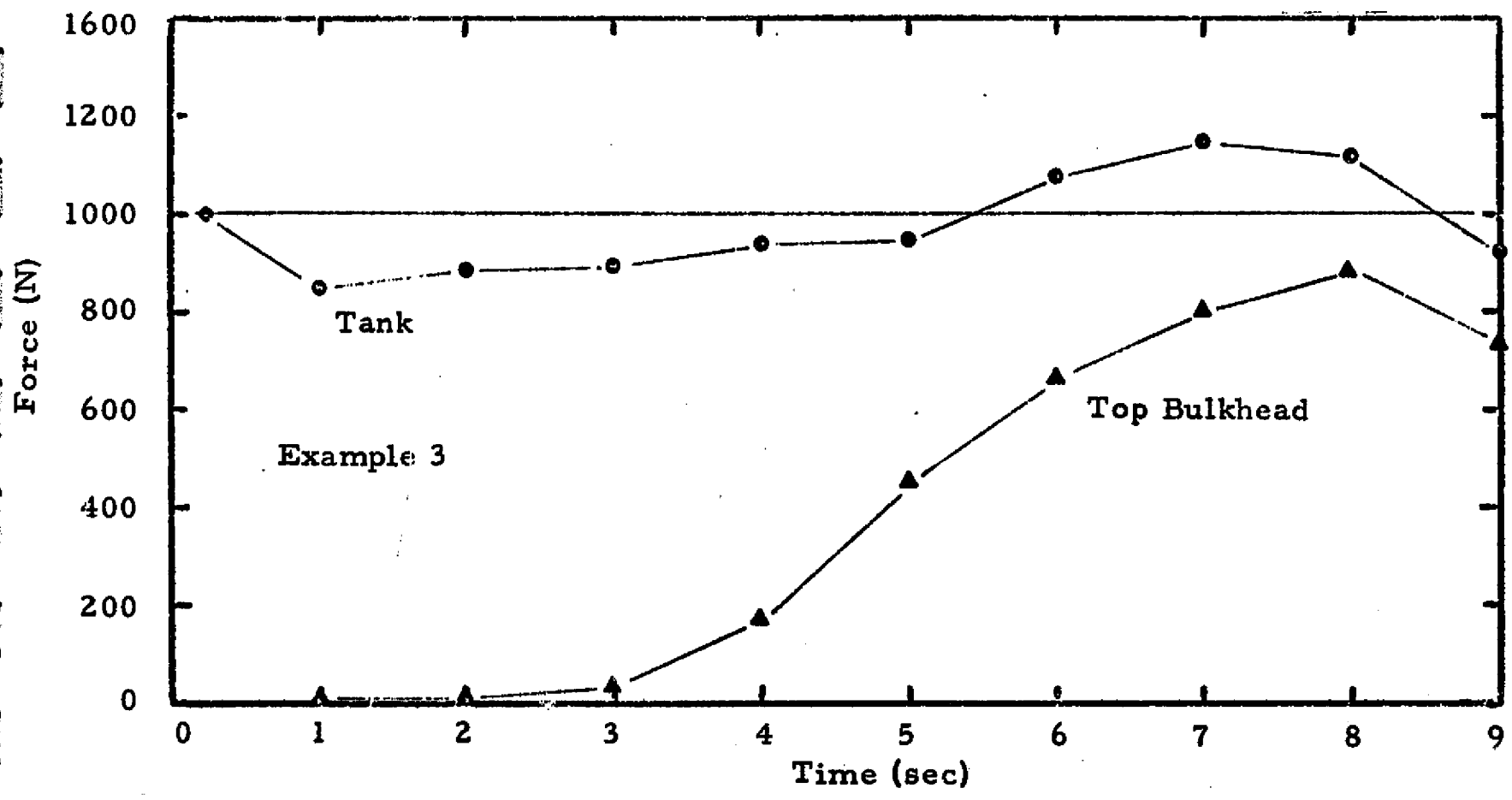

Fig. 34 - Force Exerted by the Liquid on the Container (Sample Problem I)

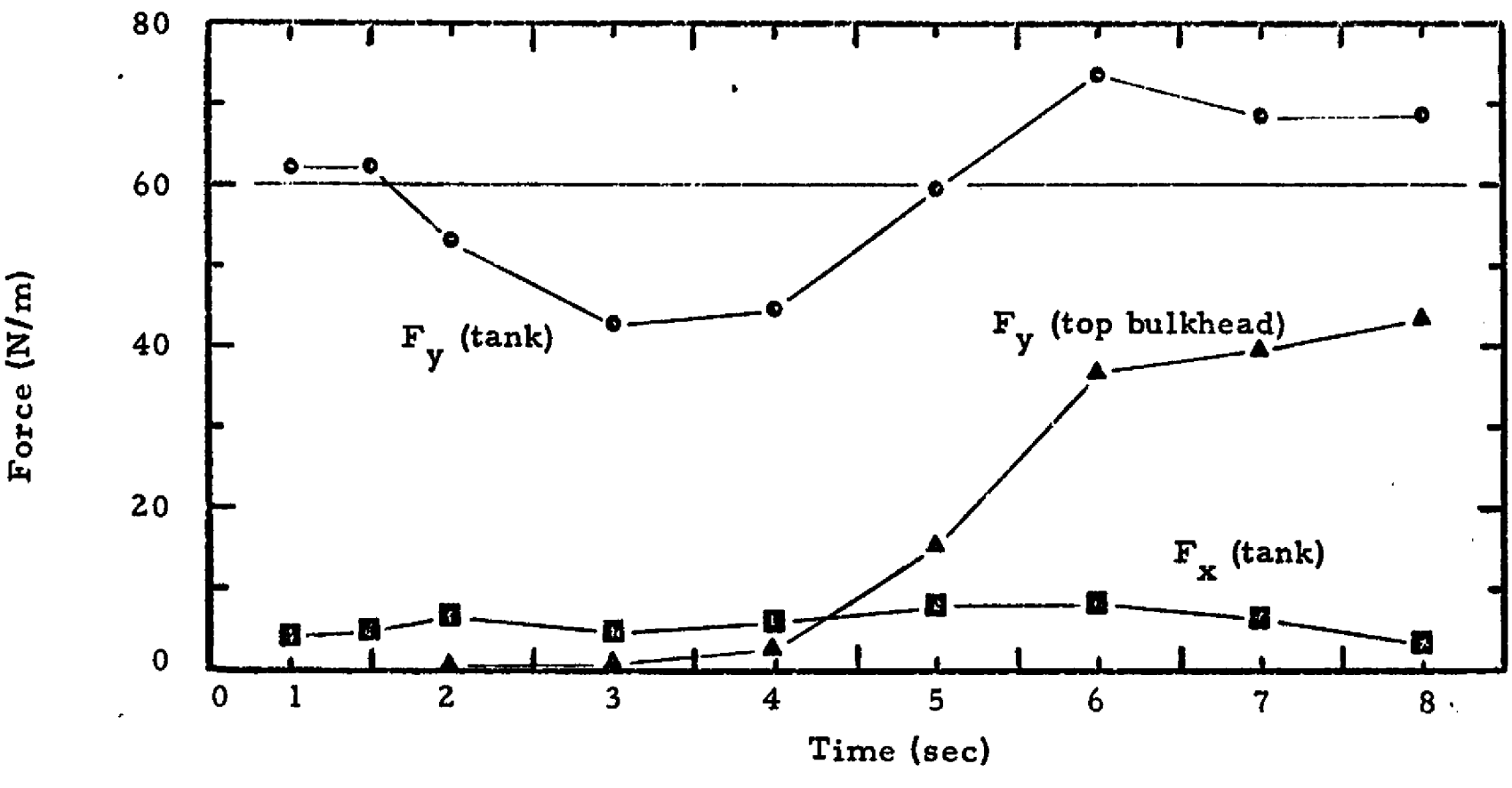

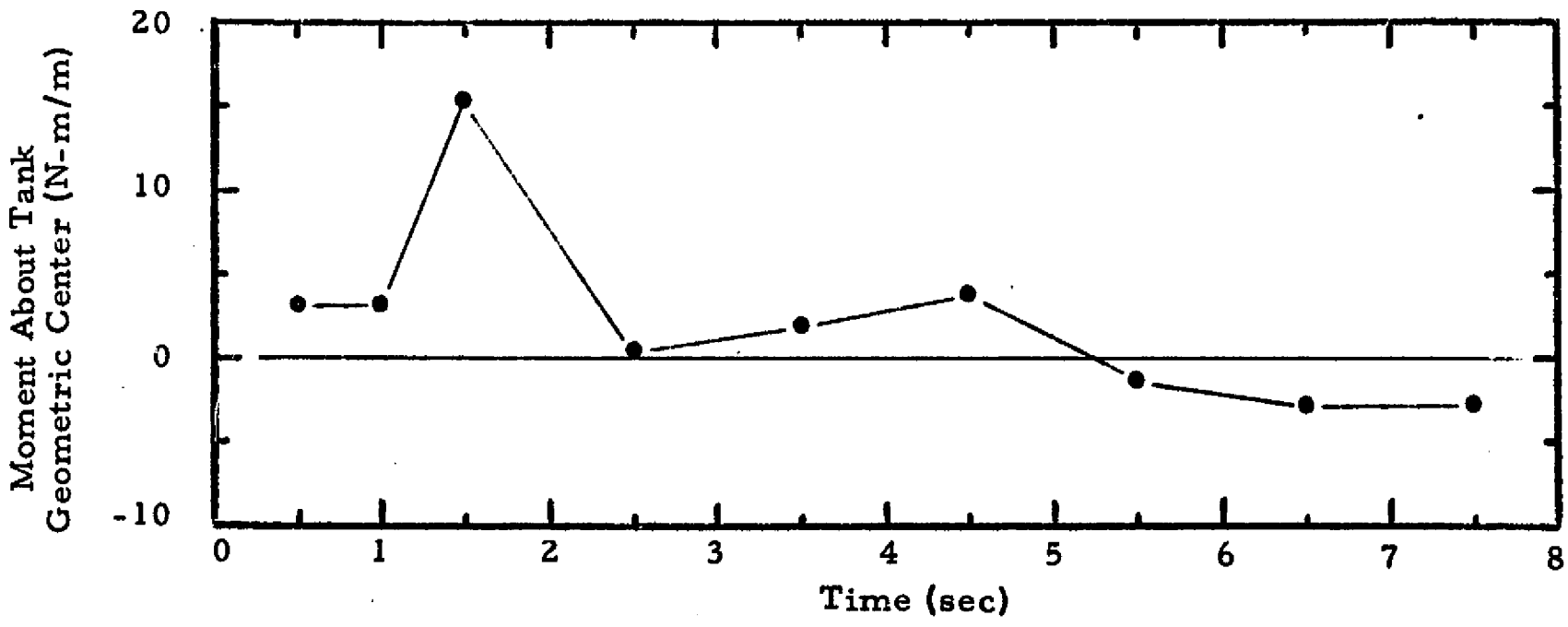

Example 3

Fig. 35 - Forces and Moment Exerted by the Liquid on the Container (Sample Problem II)